REPUBLIC OF TURKEY

ACIBADEM MEHMET ALİ AYDINLAR UNIVERSITY

INSTITUTE OF HEALTH SCIENCES

ENHANCED PHAGOCYTOSIS OF CAR MACROPHAGE IN SOLID TUMOR

DİDEM ÇAKIRSOY

MASTER THESIS

DEPARTMENT of MEDICAL BIOTECHNOLOGY

SUPERVISOR

Assoc. Prof. Özden Hatırnaz Ng

Co-Supervisor

Prof. Dr. Ercüment Ovalı

İSTANBUL-2021

REPUBLIC OF TURKEY

ACIBADEM MEHMET ALİ AYDINLAR UNIVERSITY

INSTITUTE OF HEALTH SCIENCES

ENHANCED PHAGOCYTOSIS OF CAR MACROPHAGE IN SOLID TUMOR

DİDEM ÇAKIRSOY

MASTER THESIS

DEPARTMENT of MEDICAL BIOTECHNOLOGY

SUPERVISOR

Assoc. Prof. Özden Hatırnaz Ng

Co-Supervisor

Prof. Dr. Ercüment Ovalı

İSTANBUL-2021

DECLARATION

This thesis is my work, from the planning to writing of the thesis that I have no unethical behavior at all stages from the planning to the writing of the thesis that I have obtained all the information and interpretations not obtained by this thesis. That I have cited all the information and comments that were not obtained through this thesis study, and that I have included these sources in the list of resources and declare that I am not infringing any patents or copyrights at the time of writing.

08.07.2021
Didem Çakırsoy

ACKNOWLEDGEMENT

I would like to express my thanks to my supervisors. First of all, Assoc. Prof. Özden Hatırnaz Ng, for believing in me, trusting me, and always opening her door to me. Secondly, I am honored to take a part in Prof Dr. Ercüment Ovalı's R&D and being the little "Didi" of the team. I would like to thank him for being as excited as I was when I presented my project idea to Mr. Ovalı and for supporting me financially and morally. I am grateful for his trust in me for enabling me to grow and develop and for all the values it has given me. I would like to express my special thanks to my all-time mentor, Assoc. Prof Yuk Yin Ng, who always helps me and stands behind me every time I reach a dead-end, and I am grateful for his presence. I realize the advantages of going through his education and discipline every day. I want to thank each member of the Acıbadem Labcell R&D team for their help and motivation. Also, Cihan Taştan, Ph.D. for guiding and encouraging me at the starting point of the project. I owe a big thank to my older sister, Dilan Aytaç, for constantly motivating me with her presence and trust. I'd want to thank my family for their unwavering support and unconditional love. I'd like to express my gratitude to Assoc.Prof. Devrim Öz Arslan for supplying the U937 cell line that was used in this study.

TABLE OF CONTENTS

LIST OF TABLES

LIST OF FIGURES

LIST OF SYMBOLS AND ABBREVIATIONS

α	Alpha
ATCC	American Type Culture Collection
ADCC	Antibody-Dependent Cell-mediated Cytotoxicity
B-ALL	B-Cell Acute Lymphoblastic Leukemia
CO2	Carbon Dioxide
CTV	Cell Trace Violet
°C	Celsius
CAR	Chimeric Antigen Receptor
CD	Cluster of Differentiation
CBA	Cytokine Bead Array
DC	Dendritic Cells
DNA	Deoxyribonucleic Acid
DLBCL	Diffuse Large B-cell Lymphoma
DMEM	Dulbecco's Modified Eagle Medium
DPBS	Dulbecco's Phosphate-Buffered Saline
EGFR	Epidermal Growth Factor Receptor
FBS	Fetal Bovine Serum

G	G-force
g	Gram
Gy	Gray
HBV	Hepatitis B Virus
HCV	Hepatitis C Virus
hr	Hour
HIV	Human Immunodeficiency Virus
HSA	Human Serum Albumin
INRG	International Neuroblastoma Risk Group
KIR	Killing Inhibitory Receptor
LAL	Limulus Amebocyte Lysate
MSC	Mesenchymal Stem Cells
µl	Microliter
ml	Mililiters
mg	Milligram
MOI	Multiplicity Of Infection
ng	Nanogram
NK	Natural Killer
NCC	Neural Crest Cells

%	Percentage
PBMC	Peripheral Blood Mononuclear Cells
RCL	Replication competent lentiviruses
rpm	Revolutions per minute
Th	T Helper
FDA	The Food and Drug Administration
TEM	Transmission Electron Microscopy
TSA	Tryptic Soy Agar
TIL	Tumor Infiltrate Lymphocytes
TME	Tumor Microenvironment
TNFR	Tumor necrosis factor receptor
VDRL	Venereal Disease Research Laboratory
ζ	Zeta

SUMMARY

The most common solid tumor in childhood is neuroblastoma, and the survival rate in high-risk groups is quite low. GD2 is a surface antigen that has overexpression in neuroblastoma. Therefore, GD2 is suitable for targeted antitumor therapies. Chimeric antigen receptor (CAR) was developed to transduce the immune cells against tumors. CARs are synthetic receptors, which designed to target specific tumor antigen. CAR T cell therapy has proven to be effective for hematological malignancies but solid tumors present significant difficulties. Macrophages have an advantage against solid tumors like; phagocytosis, triggering immunity by presenting tumor antigens and penetrate the tumor. The CAR NK-92 concept, widely used in immunotherapy, has great potential in terms of low toxicity. Hassasin, patented product of Acıbadem Labcell, was produced by transducing the NK-92 cell line and CD16 expression was provided as well as IL-12 secretion. In addition to primary macrophages and NK-92 cells, U937 emerges as a cell group that can effectively differentiate into macrophages and has anti-tumoral effects. In this study, a 2nd generation CAR was designed against the GD2 antigen and transduced in primary M1 Macrophage, NK-92, Hassasin, U937 cell groups, and in vitro efficacy studies were carried out. GD2 CAR U937 was the most effective cell line in terms of tumor-killing capacity, immune system stimulation, ease of production, standardization of effectiveness, circulation time in the body. In conclusion, the GD2 CAR U937 cell line has the potential to be successful in GD2 positive solid tumors and is a suitable candidate for clinical application.

Keywords: GD2 neuroblastoma, Immunotherapy, Chimeric Antigen Receptor, NK-92, U937.

ÖZET

Solid Tümörlerde CAR Makrofajların Artırılmış Fagositotik Etkisi

Çocukluk çağı tümörlerinde en sık görülen solid tümör nöroblastomdur ve yüksek risk gruplarında sağ kalım oranı oldukça düşüktür. GD2, nöroblastom gibi nöroektodermal kökenli tümör hücrelerinde aşırı ekspresyonu olan bir yüzey antijenidir. Bu nedenle, GD2, hedefli antitümör tedavileri için iyi bir hedeftir. Kimerik antijen reseptörü (CAR), spesifik tümör antijenini hedeflemek için tasarlanmış sentetik reseptörlerdir. Her ne kadar hematolojik maligniteler için CAR T hücre tedavisinin etkili olduğu kanıtlanmış olsa da solid tümörlerde aynı başarı gözlenmez. Makrofajlar, tümörleri fagosite etmenin yanı sıra tümör antijenlerini sunarak bağışıklığı tetiklerler. Makrofajlar tümöre sızabilme özelliğine sahiptir ve bu nedenle solid tümörlerde CAR efektör hücre olmaları açısından avantajlıdırlar. Ayrıca immünoterapi alanında yaygın olarak çalışılan CAR NK-92 konsepti, düşük toksisite riski açısından büyük potansiyele sahiptir. Acıbadem Labcell'de NK-92 hücre hattının etkinliğini artırmak için patentli bir ürün olan Hassasin geliştirildi. NK-92 hücre hattından farklı olarak bu hücrelerde, IL-12 salgılanmasının yanı sıra CD16 ekspresyonu da sağlanmıştır. U937, makrofajlara etkin bir şekilde farklılaşabilen ve anti-tümör etkileri olan bir hücre serisidir. Solid tümörlerde fagositozun önemi göz önüne alındığında, U937 CAR tabanlı hücresel genetik tedavi için büyük potansiyele sahiptir. Bu çalışmada, GD2 antijenine karşı 2. nesil bir CAR tasarlanmış ve primer M1 Makrofaj, NK-92, Hassasin, U937 hücre gruplarında transdüksiyon yapılmış ve GD2 CAR U937 hücre hattının, tümör öldürme kapasitesi, bağışıklık sistemi uyarımı, üretim kolaylığı, etkinliğin standardizasyonu, vücuttaki dolaşım süresi açısından değerlendirildi ve en etkili hücre serisi olduğu belirlenmiştir. Sonuç olarak, GD2 CAR U937 hücre hattı, GD2 pozitif solid tümörlerde başarılı olma potansiyeline sahiptir ve klinik uygulama için çok uygun bir adaydır.

Anahtar Kelimeler: GD2 Nöroblastoma, İmmünoterapi, Kimerik Antijen Reseptörü, NK-92, U937.

1. BACKGROUND AND AIM OF THE STUDY

The most common solid tumor among childhood tumors is neuroblastoma, and unfortunately, the survival rate in high-risk groups is quite low. After surgery, high-dose chemotherapy, radiotherapy, stem cell transplantation, and tumor-specific monoclonal antibody treatment options are applied to the cases in this group.

GD2 is a surface antigen and although it has limited expression on neurons, melanocytes, and peripheral pain fibers in normal tissues, its overexpression as a surface antigen is encountered in tumor cells of neuroectodermal origin such as neuroblastoma and melanoma. Therefore, GD2 is a very good target for targeted antitumor therapies (1).

Cancer cells have developed strategies such as escaping from the immune system and manipulating it to their detriment, as well as their ability to multiply indefinitely. These features they develop provide an opportunity to hide and escape from their immune system warrior cells (2). Studies focused on solving this situation, and with the help of genetic engineering, they designed receptors that recognize specific antigens carried by tumor cells. These receptors were transduced into immune cells, providing specific antitumoral effects and increased immune response.

Extracellular ligand-binding domains are linked to intracellular co-stimulatory and activation domains in CARs, which are synthetic receptors (2). In the treatment of hematological malignancies, chimeric antigen receptor (CAR) T cell therapy has proven to be effective (3). When compared to liquid tumors, solid tumors present significant difficulties for CAR-T cell therapy. High antigen heterogeneity in solid tumors provides them with an effective method of escape from CAR-T cells, which is one of the hurdles to the success of cell therapy against solid tumors (3,4). Another

significant issue for CAR T cell treatments to properly target solid tumors is that solid tumors are frequently surrounded by physical barriers that effectively inhibit T cell penetration. Another significant issue for CAR T cell treatments to properly target solid tumors is that solid tumors are frequently surrounded by physical barriers that effectively inhibit T cell penetration (5). T cells also encounter immunosuppressive tumor microenvironments (TMEs) with cellular, molecular, and metabolic characteristics that eventually lead to T cell fatigue and malfunction, which is a significant barrier for successful targeting of solid tumors with CAR T cell treatments. Solid tumors can be heavily invaded by many cell types that enable tumor development, angiogenesis, and metastasis, unlike many hematological malignancies that lack immune suppressive mechanisms (5). CAR-T cells have thus far been insufficient to overcome the extra challenges provided by solid tumors (4).

Macrophages are immune cells that absorb and consume foreign material, such as cancer cells. Activated macrophages can also aid in the promotion of an adaptive antitumor immune response since they are professional antigen-presenting cells. CAR T cells are physically rejected or inactivated, but macrophages are uniquely capable of entering solid tumors. This implies that CAR-T cell-based treatments might benefit from the addition of modified macrophages.

Natural killer (NK) cells, in addition to CAR-T cells, are potential alternative effectors that can be coupled with CAR technology. NK cell line NK-92, unlike T cells, may be used as an off-the-shelf therapy option with a lower risk of toxicity (6).

To increase the effectiveness of the NK-92 cell line, a patented product, Hassasin, was developed at the Acıbadem Labcell Cellular treatment center. Unlike the NK-92 cell line, these cells were transduced with lentiviral vectors and CD16 expression was provided as well as IL-12 secretion. With the activation of adaptive

immunity in the presence of IL-12, a more effective tumor-killing capacity is obtained.

Based on the previous clinical applications of CAR NK-92, whose phase studies are still ongoing, it was predicted that the tumor burden would be reduced by providing an effective immunity with the application of GD2-specific targeting CAR construct to the Hassasin group.

In addition to primary macrophages and NK-92 cells, U937 emerges as a cell group that can effectively differentiate into macrophages and has anti-tumoral effects. Considering the importance of phagocytosis in solid tumors and the properties of U937, it has potential for CAR-based cellular genetic therapy.

In this thesis study, in vitro analyses were performed to have pre-clinic data, the most effective effector cells which enhanced with 2nd generation GD2 CAR construct against BE(2)C, a GD2 neuroblastoma cell line. In this context, M1 GD2 CAR macrophages produced from PBMC, GD2 CAR NK-92, GD2 CAR hassasin cell groups were investigated and reported on their anti-tumor capacities, triggered immune response, ease of production, sterility.

2. INTRODUCTION

2.1. Cancer

Cancer is the general name of a large group of diseases, caused by the combination of genetic and environmental factors. Cancer is the second cause of death in the World, with an estimated number of more than 12.7 million cases impacting both men and women equally. By 2030, this number is predicted to increase to 21 million (7). In adult men lung, prostate, colorectal, stomach, and liver cancer, and in adult women breast, colorectal, lung, cervical, and thyroid cancer are the most common types of cancers. Cancer can occur at any age and affect any type of tissue. One of these tissues is the brain and the most common cancer among infants is neuroblastoma, which is the cancer of the nervous system.

2.2. Neuroblastoma

Neuroblastoma is an embryonic tumor of the nervous system and is assumed to be generated from an immature precursor cell produced from neural-crest tissues. Neuroblastomas are the most common cancer in very young children, as one might anticipate for a disease of growing tissues. The average age of children diagnosed with neuroblastoma is under 4 years old. When the tumor development process in the patient is examined, masses are usually found in the neck, abdomen, or pelvis region because this tumor model arises in the tissues of the sympathetic nervous system, typically the adrenal medulla or paraspinal ganglia (8,9).

2.2.1. Incidence

Considering the age-standardized annual case rate, the incidence of neuroblastoma for children between 0-14, is approximately 14 children per million. Statistical studies have shown that 85% of children diagnosed with neuroblastoma are younger than five years old, while 40% are in infancy. After the age of ten, they are quite rare (10,11). At the time of diagnosis, over half of the cases had distant metastases. In most infants (almost a quarter of cases under one year of age) the disease progresses with a severe pattern. These infants have distinct metastatic lesions that evade different organs, especially the skin, liver, and bone marrow (10,12).

2.2.2. Survival

When the survival rates of these patients were examined, differences were found depending on the geography. It has been reported in the most recent studies that the five-year survival rate of patients in Southern and Eastern European countries is 59 % (11).

2.2.3. Etiology

Since neuroblastoma cases are observed less frequently than leukemia or lung tumors, studies are limited. Neuroblastoma can arise in the context of malformation syndromes or genetic disorders, as well as predisposing constitutional alterations in rare cases. In the literature, genetic studies for low-risk low-penetration susceptible

alleles are still uncommon, and neither gene surrounding interactions nor epigenetic impacts of the environment have yet been addressed (11).

2.2.4. Symptoms and diagnosis

Patients with neuroblastoma may experience fatigue, fever, pain, weight loss, loss of appetite, diarrhea, irritability, or memory loss. The location of the tumor and the place of its metastasis determine the specific symptoms. In cases where abdominal masses occur, the patient may not have any symptom findings, besides, symptoms such as abdominal pain and swelling may be observed due to the pressure in the abdominal region. Tumor extension into the epidural or intradural region occurs in 10–15 percent of patients with neuroblastoma, which can cause spinal cord compression and paraplegia. In cases of neuroblastoma, spread to the orbital bones is often observed, followed by periorbital ecchymosis (raccoon eyes) and proptosis, and ultimately loss of vision. Infants are more likely to develop tumors in the cervical or thoracic areas, which can cause Horner syndrome and respiratory problems. In children diagnosed or suspected of neuroblastoma, CT or MRI imaging is used to determine the size of the primary tumor and its spread to the surrounding tissues. In addition to these, imaging of the chest and pelvis regions to determine the metastasis sites plays an important role in determining the stage of the disease (13).

2.2.5. Tumor types

A neural crest is a form of transitory cell that emerges from the closed neural tube during development. Neural crest cells (NCCs) undergo an epithelial-to-mesenchymal transition during embryo development and NCCs can move to distant sites after this transition (Figure 1). NCCs can differentiate into a wide range of cell groups that will provide the anatomical structure of the embryo in embryogenesis.

We can include neurons, glia pigment cells, and bone cells in these cell groups. In addition to being a disease originating from the neural crest-derived cells of neuroblastoma, some cases are also associated with other neural crest-derived pathologies called neurocristopathies. In these diseases, an abnormally high presence of neuroblastic tumors is observed compared to the general population. One such type of development also applies to type 1 neurofibromatosis, a well-known condition characterized by a predisposition to a wide range of tumors. Also known as Ondine's curse. The disease Ondine's curse is defined by respiratory arrest during sleep and a reduced or non-existent reaction to hypercapnia (11).

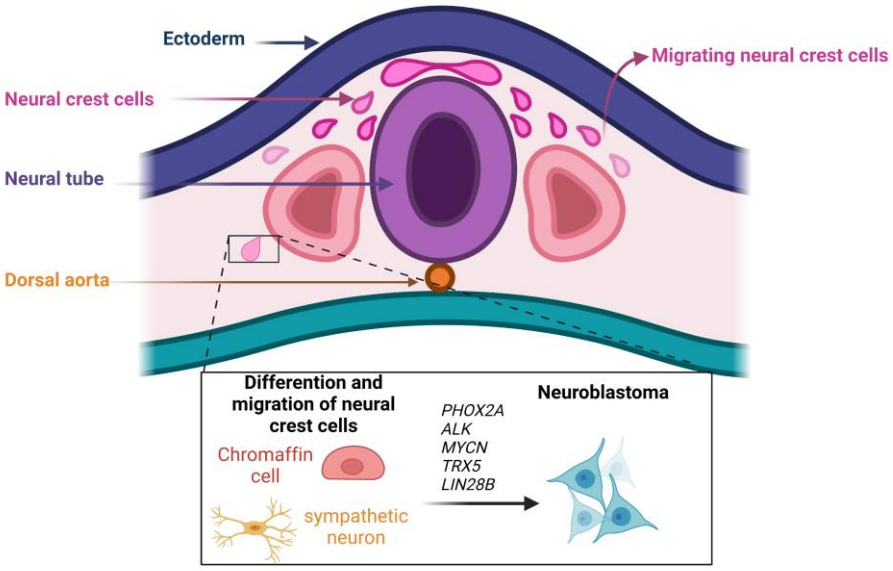

Figure 1: The process of formation of neuroblastoma from neural crest cells (14).(Created with BioRender.com)

2.2.6. Key genes involved in neuroblastoma pathogenesis

Childhood cancers possess fewer genetic aberrations than adult cancers. Next-generation sequencing analysis revealed some genetic variations in neuroblastoma as well but there is no single gene mutation that can explain all neuroblastoma cases. The *PHOX2B* gene is the main regulatory gene for the development of the autonomic nervous system consisting of ganglia. Heterozygous germ-line mutations in this gene are detected in patients diagnosed with the Ondine's curse. *MYC* proto-oncogene has very limited expression in healthy cells and is a gene that has an important role in nervous system development. Increased *MYC* gene amplification is an important diagnostic marker in neuroblastoma. Amplification of the *MYC* proto-oncogene is closely linked to advanced disease, treatment resistance, and poor outcome and is found in around 22% of neuroblastoma patients and 40% of advanced cases. Following the finding of germ-line and somatic activating mutations in a fraction of familial and sporadic cases, the *ALK* (Anaplastic Lymphoma Kinase) gene was identified as a significant neuroblastoma gene in 2008. Repetitive rearrangements and/or mutations leading to loss of somatic function of *ATRX* and overexpression of *TERT* have been detected by whole-genome sequencing of neuroblastoma cell lines and tumors (15,16). This genetic heterogeneity also brings high challenges especially in terms of treatment.

2.2.7. Risk stratification

Several predictive variables linked with patient outcomes have been established due to the biological and clinical heterogeneity of neuroblastoma tumors. A better understanding of clinical and biological risk factors is essential when developing neuroblastoma treatment strategies, which has let treatment classification increasingly important. The patient's age, tumor size, histology, DNA ploidy, *MYCN*

expression level, cytogenetic factors, and markers in the serum can be considered as the prognostic factors. Clinical heterogeneity is the most basic condition encountered in neuroblastoma. Considering a variety of clinical and biological factors, patients are assessed as low, intermediate, or high risk. Risk groups were determined through the International Neuroblastoma Risk Group (INRG) categorization system, and it was aimed to treat patients more consciously. The treatment options are chosen according to these risk groups; children with the low-risk disease can be observed or operated, while those with the moderate-risk disease can receive chemotherapy and surgical resection. Children with high-risk diseases receive intensive, the multimodal treatment that includes chemotherapy, surgery, autologous stem cell chemotherapy, radiation, and immunotherapy (17).

2.3. Disialogaglioside (GD2)

GD2 is the surface antigen, which is a ganglioside located at the outer membrane of all neuroblastomas. Although the biochemical structure of GD2 ganglioside is complex, it is in the form of an acidic glycolipid. GD2 expression is limited to normal tissues, peripheral neurons, the central nervous system, and skin melanocytes. Neuroblastoma cells have an increased expression of GD2 and enzyme activity. GD2 is expressed in a range of embryonal cancers, including brain tumors, retinoblastoma, Ewing's sarcoma, osteosarcoma, and rhabdomyosarcoma (18). Although it is thought to play a role in neural differentiation and repair, the role of GD2 in normal development has not been fully explained. As the common purpose of gangliosides, including GD2, can act as receptors for microbial toxins together with that they have a function to mediate cell adhesion. The increase of GD2 expression level in breast cancer stem cells provided evidence for the association of GD2 with tumorgenicity. While the increased GD2 level suppresses the immune cells by showing an immunosuppressive effect against the effector cell group, it also causes an increase in the mobility of the cell, which increases the risk of metastasis (18,19). The National Cancer Institute's cancer antigen prioritization program has garnered attention for the

development of GD2-targeting therapies, placing GD2 in the 12th top cancer antigen list (20). Tumor development and rate are directly related to the number of tumor gangliosides present. Patients diagnosed with neuroblastoma with high circulating GD2 levels have a shorter average survival rate of 9 months compared to patients with low GD2 levels (12).

2.3.1. GD2 Neuroblastoma treatment options

In the treatment of patients, circulating GD2 levels decrease as a positive response during the treatment and rise again in patients with recurrent tumors (12). In vivo and in vitro studies have shown that free circulating tumor gangliosides inhibit specific immune reactions. It creates an immunosuppressive effect by inhibiting T cell proliferation and immune system responses via IL-2 suppression (13). According to studies, for patients with high-risk neuroblastoma, long-term survival rates are currently approximately 40–50 percent (8). Effective treatment options for patients with advanced neuroblastoma are very limited and, as a result, the mortality rate is high in patients. The standard treatment protocol for advanced cases includes high-dose chemotherapy, surgery, and radiation (15).

2.4. Immunotherapy

One of the most encouraging areas of cancer research and clinic is cancer immunotherapy. Fundamentally, cancer immunotherapy is to allow the patient's immune system to realize the cancer cells as invaders and show reactions against them. The main target for neuroblastoma immunotherapy is GD2. Unituxin, Dinutuximab-beta, are FDA-approved specific monoclonal antibodies targeting GD2 and are used to treat high-risk patients. Studies have shown that Dinutuximab-beta is

effective and when used in the treatment of high-risk patients, it increases the survival rate (13).

2.5. Chimeric antigen receptor (CAR)

Our immune system is continuously on the lookout for malignant cells and dangerous bacteria in our bodies. Because it detects certain signals on the surface of hazardous cells, it can detect these risks. Cancer cells, on the other hand, frequently develop ways to evade our immune system (21). Cancer cells have developed strategies to skip immune control and proliferate indefinitely. As a result of these features, they are not noticed and overcome the attacks of immune cells (2). To solve this problem, genetic engineering techniques were used to modify immune cells to express designed receptors that specifically recognize antigens through the use of extracellular cell-binding domains and then activate immune effector mechanisms via intracellular signaling cascades (22).

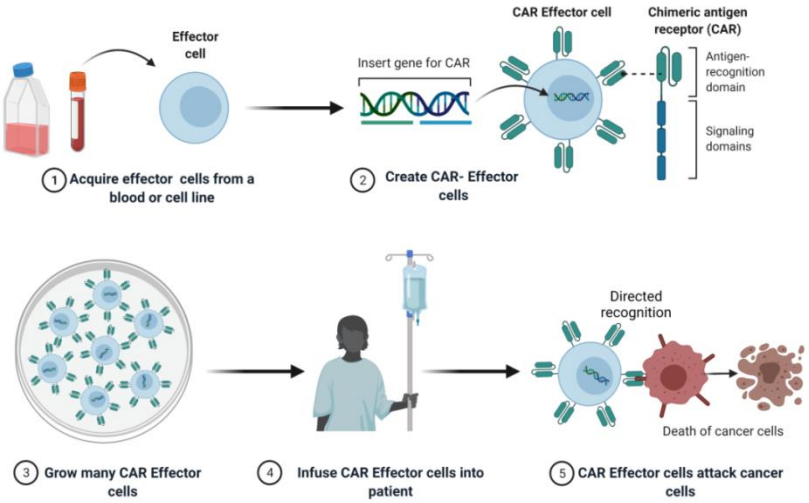

Figure 2: Key steps in CAR effector cell generation and strategy.
(Created with BioRender.com)

CAR-T cell immunotherapy is already being utilized to treat blood cancer patients and has shown a lot of success in the treatment of hematological malignancies (Figure 2). CD19 antigen is the most researched therapeutic target (22,23). There are two CD19 specific CAR-T cell products approved by the FDA. Kymriah targets B cell acute lymphoblastic leukemia (B-ALL), while Yescarta targets diffuse large B-cell lymphoma (DLBCL) (24,25).

2.5.1. The perspective of solid tumor

CAR-T cell therapy has proven effective for hematopoietic malignancies. However, it is not effective in diffuse into and killing solid tumors, which restricts its application (Figure 3) (6,23). In the most promising trials in solid tumors, only 3 out of 11 patients treated by the CAR-T against GD2 neuroblastoma achieved cure with complete remission (26). Considering the underlying causes of the failure of CAR-T cellular therapy in solid tumors, new strategies may be found that can be successful in this area. CAR-T cell is more likely to encounter hematological cancer cells compared to solid tumors. CAR-T cells must first travel to tumor locations to attach to their target proteins on the tumor's surface. This is a necessary condition for T cell immunotherapy to be effective T cells that enter solid tumor sites are often greatly suppressed by the immunosuppressive microenvironment, a situation not encountered in hematological malignancies. In addition, chemokines secreted from solid tumors such as CXCL1, CXCL12, and CXCL5 inhibit T cells from entering the tumor site (27). Hypoxia, low pH, immunological suppressor cells, an increase in inhibitory checkpoints, and increased tumor-derived cytokines are all inhibited CAR-T cells (6,23,28).

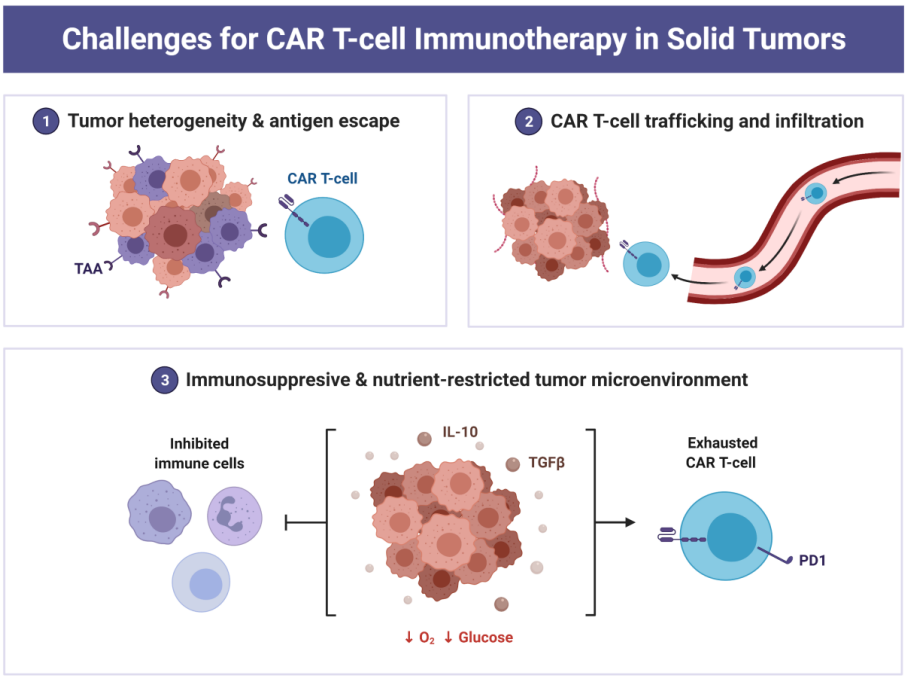

Figure 3: Challenges for CAR-T cell immunotherapy in solid tumors. (Created with BioRender.com)

Few trials have been developed to activate the myeloid part of the immunity to combat cancer, instead of the adaptive immune system. Granulocytes and monocytes, which can develop into macrophages or dendritic cells, make up the myeloid immune lineage. When the tumor microenvironment is examined, the density of macrophage cells draws attention. This presents a new perspective for immunotherapeutic drug development (29).

2.6. Macrophage

The innate immune system mechanism is developed to defend the body against infections, allergies, and other foreign organisms that invade the body. Macrophages are one of the innate immune cell populations that were initially characterized in

1882 by Elie Metchnikoff as cells involved in the phagocytosis of foreign particles. Macrophages that arise from PBMC (peripheral blood mononuclear cells) may be found in nearly every tissue and organ system, for example, the respiratory tract, skin, gastrointestinal tract, and reproductive tract (30). Macrophages cannot only penetrate foreign cells but also activate the adaptive immune system. They are important for sustain immunological homeostasis and regulating the adaptive immune system by serving as antigen presentation cells (APCs) and delivering other signals needed for an efficient adaptive immune response to infection (31–34). Macrophages are classified into M0, M1, and M2 classes depending on their polarization status. M0 is categorized as a naïve state but when M0 macrophage encounter with pro- (LPS, Th1 cytokines) or anti-inflammatory (Th2) signal, it differentiates M1 or M2 respectively (35).

Macrophages contain various types of Fc receptors, and they have a lot of power when it comes to destroying malignancies through antibody-dependent phagocytosis. Several studies have shown that phagocytosis of macrophages is a key of activation for several cancer-fighting antibodies (36).

Most malignancies have a lot of macrophages in their TME, which trigger metastasis and angiogenesis, enable metastasis, and enhance immunosuppression (26). Considering that macrophages in the tumor microenvironment work to the benefit of the tumor, cellular immunotherapy by manipulation of macrophages has great potential.

Macrophages become active when they come into contact with a foreign organism or cancer cell. In a tumor environment, infiltrating macrophages need interferon-γ (IFNy) and tumor-necrosis factor (TNF) signals to be activated, and these signals are provided by other immune cells in the medium. As a result, the

tumor-killing capacity of the activated macrophage population increases and begins to secrete pro-inflammatory cytokines (32).

2.6.1. CAR macrophage

The phagocytotic effect of macrophages can be modulated and increased via gene engineering. In this regard, genetically modified-macrophage may be a useful clinic candidate. Macrophages that have been modified to be more targeted and have improved phagocytotic capabilities against cancer cells, as a result of phagocytosis macrophage can start a cascade of immunological responses (Figure 4) (35,37,38).

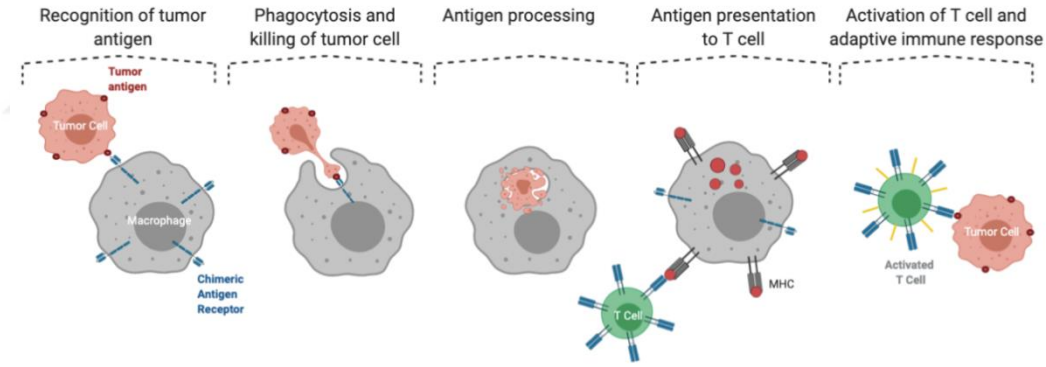

Figure 4: Function and mechanism of action of CAR macrophage (39).

Human macrophages expressing CARs might reroute their phagocytic activity, resulting in a specific antitumor therapeutic impact with the capacity to trigger adaptive immune cells. Morrissey et al. developed a CAR model and expressed it into macrophages. Engineered macrophages were able to detect and destroy the target, as well as pointing the potential to bite cancer cells and restrict their growth. In support of these results, the team demonstrated that in vivo studies significantly reduced tumor burden create a pro-inflammatory tumor microenvironment and

increase anti-tumor T cell activity while prolonging the survival time of mice (34,40).

2.7. NK-92- Hassasın

Natural killer (NK) cells are lymphocytes and are one of the important elements of the immune system. The presence of the cell adhesion marker CD56 and the absence of the T-cell receptor CD3 distinguish natural killer (NK) cells. Recent studies have shown that NK cells have the potential to transform into another highly potent effector cell group with engineered CARs and achieve success in immunotherapy (41). Primary NK cells, on the other hand, might be difficult to identify and grow in the laboratory, and their therapeutic efficacy can be easily influenced by subset ratios and phenotypic characteristics. Considering such disadvantages of NK cells, clinical applications of NK-based cell lines such as NK-92 are quite advantageous. Especially the NK-92 cell line preserves its phenotypic characteristics and can be produced in very high numbers in the presence of IL-2 cytokine. Except for a lack of FcRIII (CD16) expression, NK-92 has comparable features to activated peripheral blood NK cells and they were obtained from a non-Hodgkin lymphoma patient (6,42).

NK-92 is a group of cells that produce a cytotoxic reaction response by expressing high levels of perforin and granzyme B cytolytic pathway molecules. This cell group does not express any form of the Killing Inhibitory Receptor (KIR) family and is naturally immune to this manipulation of the cancer cell. CAR design studies on the NK-92 cell line have been studied before. The therapeutic effects of CAR-NK-92 cells produced specifically for antigens such as CD19, CD20, and HER2 are being studied. Safety is a top priority when using a cell line as a therapeutic agent, so in clinical studies, NK-92 cells have been irradiated and infused safely (6). Although it may seem paradoxical to infuse cancer cells, studies show that it is safe as long as

the cells are irradiated before infusion. In vivo growth is inhibited by irradiation, but the cells' capacity to destroy target cells and generate immune-active cytokines is preserved. After irradiation with 1000 cGy, which suppresses growth, functional cytotoxicity is preserved in NK-92 (42,43).

2.7.1. IL-12

Interleukin-12 (IL-12) is one of the important cytokines for the immune system. When a foreign organism is encountered, IL-12 produces phagocytic cells, B cells, and dendritic cells and stimulates T cells and NK cells by increasing the activity of cytotoxic lymphocytes (CD8) and inducing cytokines such as IFN- γ. IFN- γ is a very important cytokine for the anti-tumoral response, and T helper 1 cells that produce IFN- γ begin to form thanks to IL-12 (43,44). In addition to these, IL-12 has many properties such as restoring tumor infiltrate lymphocytes (TILs), inhibiting the suppression of effector T cells, and attracting NK cells to the tumor site to exert antitumor effects and regulate the tumor environment (43).

2.7.2. CD16

Through the Fc component of IgG, the CD16 receptor facilitates antibody binding. When combined with tumor-targeting antibodies, this characteristic allows NK cells to kill through an extra mechanism known as antibody-dependent cell-mediated cytotoxicity (ADCC). The CD16 (FcRIIIa) receptor is not expressed in the parental NK-92 cells. As a result, ADCC cannot be enhanced by NK-92 cells (42,45).

2.7.3. Hassasin cell line

Hassasin cell line (Figure 5) is a patented product of Labcell cellular therapy Inc. The Hassasin cell line with patent number PT2019-01624 (TR), PY2019-00456 (PCT), PY202000411 (EP) was designed, manufactured, and sold as a product by Labcell. The susceptible cell line is mainly based on the NK-92 cell line. NK-92 cells were transfected with IL-12 and CD16 gene constructs and this new cell line was named Hassasin. IL-12 expression of NK-92 cells transfected with lentivirus vector method carrying IL-12 - CD16 plasmids was proven by IL-12 Elisa method and CD16 expression was measured by flow cytometry. The transfection efficiency of the population was increased by sorting CD16. The quality of the cell line has been shown in the cytogenic and sterility parameters and it has been shown with repeated passages that there is no cytotoxic effect.

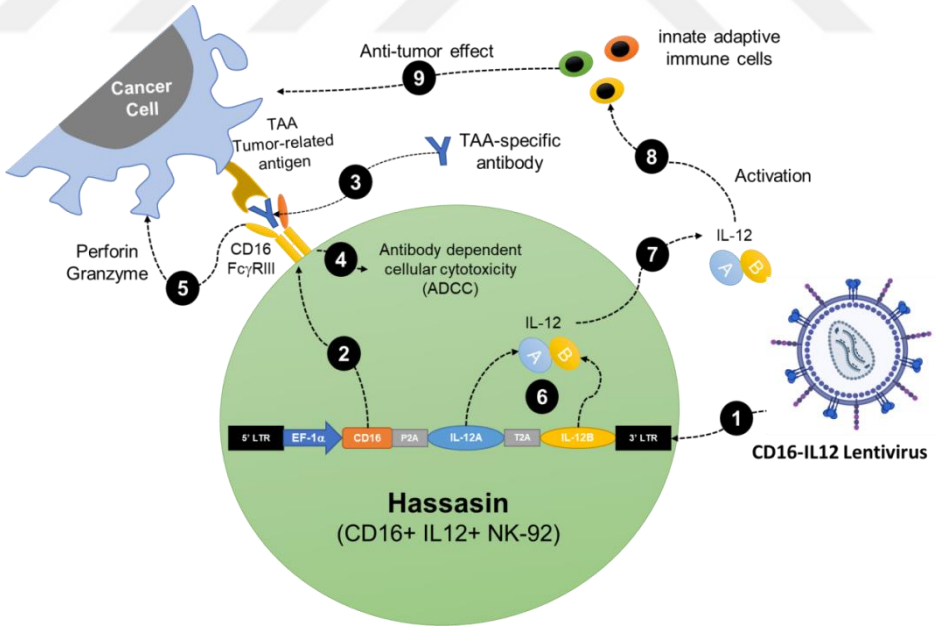

Figure 5: The design mechanism and action pathways of the Hassasin cell line.

The CAR construct was assembled into the Hassasin cell group by transfection with a second lentiviral vector and targeted directly to the tumor cell group. In vitro, in vivo projects aiming to measure the tumor-killing capacity and the adaptive and innate/immune system stimulation with IL-12 by attaching antigen-specific CAR constructs of CD19, BCMA, GD2, MUC-1 are carried out by the Labcell R&D department.

2.8. U937 cell line

U937 is a pro-monocytic, myeloid leukemia cell line identified from the histiocytic lymphoma of a 37-year-old man. U937 is very similar in characteristic to monocytes and simple to utilize. It's possible to make an almost infinite number of cells, and they're all quite uniform (46). In previous studies, the differentiation mechanism from monocytes to macrophages was revealed by modeling the U937 cell line. Apart from this, cytotoxicity, host-pathogen interactions, cancer, and inflammation processes were studied on the U937 cell line and information about these mechanisms was gathered (47).

The U937 cell line has potential for immunotherapy because of its ease of use, its lethal effect against tumors, and its ability to differentiate into macrophages when it encounters a tumor (48).

2.9. CAR Domains

The CAR construct (Figure 6) that is designed in this study composed of a GD2 tumor-specific single-chain fragment CD8 antibody fragment fused via a hinge and

transmembrane regions to intracellular signaling moieties CD3ζ and co-stimulatory protein CD137 (4-1BB).

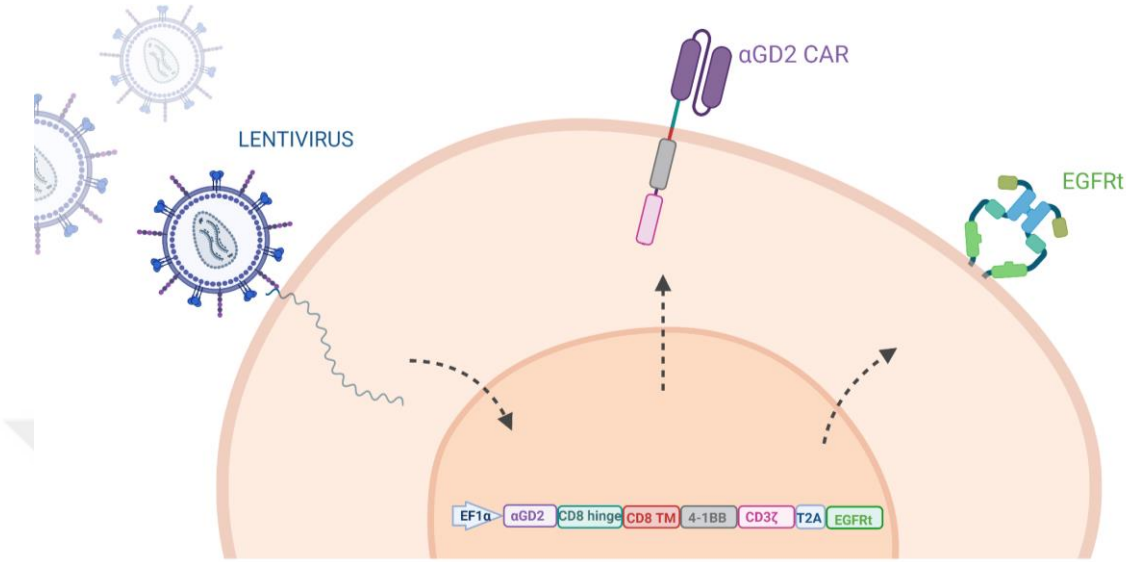

Figure 6: CAR constructs and their mechanism of action.
(Created with BioRender.com)

2.9.1. CD3ζ (zeta)

The antibody-dependent cellular phagocytosis (ADCP) features of macrophages are triggered by the FcεRI-y signal molecules and CD3ζ has the same homology as these molecules. Studies have proven that CD3ζ-based CARs increase anti-tumor phagocytic activity and trigger cytolytic activity (34,49).

2.9.2. 4-1BB

CD137 (4-1BB), a cytokine receptor, is in the TNFR family and is expressed by activated T cells. CD137 (4-1BB) ligand expressed in peripheral human monocytes

transmits T cells activating signal. Studies have shown that CD137 ligand increases the proliferation and colony formation of hematopoietic progenitor cells and their differentiation into macrophages in humans and mice. In peripheral cells such as monocytes and macrophages, the CD137 ligand signal carries signals of attachment, activation, migration, survival, and proliferation to these cells (50,51).

2.9.3. EGFRt

One of the most critical aspects in genetic engineering of cellular therapeutics is the purification of the transgenic cell population by selecting cells capable of expressing the transferred genes. Thus, unnecessary, non-transgenic cells are removed from the population, increasing the therapeutic effect and safety of the product. For this purpose, many methods are being researched and used for the selection of transgenic cells. One of them, the human epidermal growth factor receptor (EGFR) is a receptor tyrosine kinase in the ErbB growth factor receptor family. Since EGFR is not expressed in cells of hematopoietic and lymphopoietic origin, it can be targeted for use in selection by giving it during gene transfer. EGFRt is created by gene engineering methods with small cuts to be created in the extracellular parts of the cell in the EGFR protein sequence and by cutting the intracellular cytoplasmic domains. Thus, while the size of the gene to be transferred decreases, EGF cannot bind to EGFRt, even if it binds, EGFR signaling cannot occur due to the absence of downstream pathways for the cell. The use of the EGFRt design with the transferred target therapeutic gene is used as a mediator in the selection of the cell population to which the therapeutic gene can be transferred (22,52).

3. MATERIALS AND METHODS

3.1. Materials

Table 1: List of cell lines and their area of usage.

Cell lines	Cat No, Brand	Area of usage
Jurkat-Acute T cell leukemia	TIB-152,ATCC	Lentiviral titration and RCL test
HEK293T- Human embryonic kidney	CRL-3216,ATCC	Lentivirus production
NK-92-Malignant Non-Hodgkins Lymphoma	CRL-2407,ATCC	CAR-Effector cell
Hassasin-CD16+IL-12+ NK-92	Acibadem Labcell	CAR-Effector cell
MSC-Mesenchymal stem cells	Umbilical cord-derived	Cytopathic effect assay on somatic cell
U937-Histiocytic Lymphoma	CRL-1593.2,ATCC	CAR-Effector cell
BE(2)C-Neuroblastoma	CRL-2268, ATCC	Target neuroblastoma cell line

Table 2: List of kits, solutions, and antibodies.

Kits, solutions, and antibodies	Cat No, Brand
RPMI 1640 medium	01-101-1A, Biological Industries
DMEM medium	11965084, Gibco
TexMACS medium	130-097-196, Miltenyi

Table 2: List of kits, solutions, and antibodies (Continue).

Heat-inactivated fetal bovine serum	10500064, Gibco
Penicillin-streptomycin (10X)	03-031-5B, Biological Industries
DPBS	02-023-1A, Biological Industries
IMDM medium	12-722F, Lonza
Isopropanol	A3928, PanReac Appli chem
MTT Solution	CT01, MercMillipore
Trypan blue	T8154, Sigma Aldrich
MACSPlex Cytokine Bead Array kit	130-099-169, Miltenyi
CD14 MicroBeads, human	130-050-201, Miltenyi
Cell Trace Violet cell proliferation kit	C34557, Invitrogen
CD14-PE	130-110-519, Miltenyi
CD206-FITC	130-123-671, Miltenyi
CD163-vioblue	130-112-134, Miltenyi
CD86-Pevio. 770	130-113-573, Miltenyi
CD4-APC. Cy7	317418, Biolegend
CD8-FITC	301050, Biolegend
CD25-APC	302610, Biolegend
CD107a-PerCP/Cy5.5	328616, Biolegend
CD56-PE	981202, Biolegend
Human Anti-EGFR Alexa Fluor 488	352908, Biolegend
Vectofusin-1	130-111-163, Miltenyi
QIAfilter Plasmid Giga Kit	12291, QIAgen
Lenti-X concentrator	PT4421-2, Takara
Fugene HD Transfection Reagent	E2312, Promega

Table 2: List of kits, solutions, and antibodies (Continue).

Optimem	31985070, Gibco
MSC NutriStem® XF Medium	05-200-1A, Biological Industries
MSC NutriStem® XF Suppl. Mix	05-201-1U, Biological Industries
Ringer Lactate	PPB-2001252, Polypharma
Human Serum Albumin	Octapharma CSL Behring
Ficoll-Paque Plus	17-1440-02, Cytiva
LB agar	110283.0500, Merck
LB broth	110285.0500, Merck
Ampicilin 100mg/mL	A5354, Sigma Aldrich
Human EGFR Biotinyleted antibody	FAB9577B-100 , R and D systems
Streptavidin Microbeads	130-048-101, Miltenyi
LS column	130-042-40, Miltenyi
MACS GMP recombinant human IL-2	170-075-14, Miltenyi
Human IL-4	130-094-117, Miltenyi
Trypsin EDTA solution C	03-053-1B, Biological Industries
Rh-GM-CSF	P04141, CellGenix
Recombinant Human IFN-gamma GMP Protein	285-GMP-100, R and D systems
Human TruStain FcX	422301, Biolegend
R-Phycoerythrin AffiniPure $F(ab')_2$ Fragment Goat Anti-Human IgG,	MOB-0239MC, Creative Biolabs
2-mercaptoethanol	21985023, Gibco

Table 3: List of the main equipment.

Main equipment	Cat No, Brand
Class II Biological Safety Cabinet	MN120, Nüve
Light microscope	Leica
Inbubator	IC0150med, Memmert
Fluorescent microscope	Zeiss Axio Scope A1
Elisa Reader	Omega, BMG
Flow Cytometer	Ctoflex, Beckman Coulter
Water bath	NB20,Nüve
Centrifuge	Allegra X-30R, Beckman Coulter
Automated cell counter	T20, Biorad
Pipette Aid	Pipetus, Hirschmann
Pipette (10, 100, 200, 1000 uL)	Axygen
Freezer (+4)	1060TY, Arçelik
Freezer (-20)	1060TY, Arçelik
Freezer (-80)	DW-86L628, Haier
MidiMACS Magentic Separator	Midi,Clinimacs
Nanodrop	NanoDrop one, Thermo

3.2. Methods

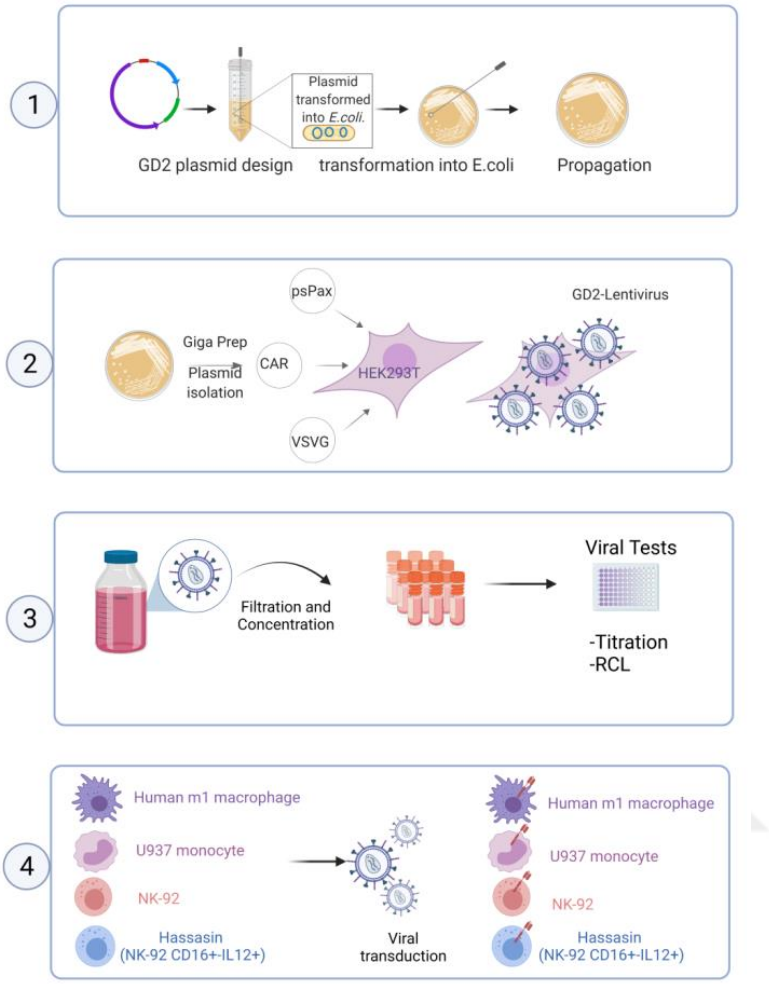

Figure 7: Flow of methodology. 1. Plasmid design and transformation. 2. Lentivirus production. 3. Lentivirrus quantification and safety tests. 4. Transduction of effector cells. (Created with BioRender.com)

3.2.1. Cell culture

In this study, the HEK293T (#CRL-3216, ATCC), Jurkat (#TIB-152, ATCC), NK-92 (#CRL-2407,ATCC), Hassasin(PT2019-01624 (TR)), the BE (2) C Neuroblastoma cell line (#CRL-2268, ATCC) and the U937 cell line (#CRL-1593.2, ATCC) cell lines were used.

All cell lines were cultured in the mediums according to their specific conditions supplemented with 10% fetal bovine serum albumin (FBS) (#10500064, Gibco), and 1% penicillin-streptomycin (#03-031-5B, Biological Industries). Cell viability was preserved by passaging and incubated at 37 °C.

MSCs (mesenchymal stem cells), obtained from the leftover samples derived from umbilical cords that were collected for bone marrow transplantation purposes, were used for testing cytopathic effect assay on somatic cells (Donor consent form is attached in appendix 1). The frozen umbilical cord-driven MSC taken from the nitrogen tank was washed 2 times with DPBS w/o 400 G centrifuge for 10 min. Pellet MSC Medium (#05-200-1A, Biological Industries) was filled with 10% FBS (#10500064, Gibco), 1% penicillin-streptomycin (#03-031-5B, Biological Industries) and MSC NutriStem® XF Suppl. Mix (#05-201-1U, Biological Industries) and cell count were taken. Total $4x10^{6}$ viable cells were planted in T300 flask in 50 ml MSC medium. Cell viability was preserved by passaging twice a week. It was placed in the incubator at 37°C.

3.2.2. GD2 CAR lentivirus production and efficacy tests

3.2.2.1. Plasmid design

The nucleotide sequence of the CAR construct's domains was obtained in a gene bank and produced by Creative Biolabs (Project no: CBLZ101118 Z2C CAR). Chimeric antigen receptors (anti-GD2 scFv from Dinutuximab) were manufactured in their entirety and sub-cloned into lentivirus vectors. Sanger sequencing was used

to validate the insertion. The structure of CAR vectors is shown schematically below in Figure 8.

"EF-1alpha promote-signal peptide-scFv-CD8 hinge-CD8 transmembrane-4-1BB-CD3zeta-T2A-EGFRt"

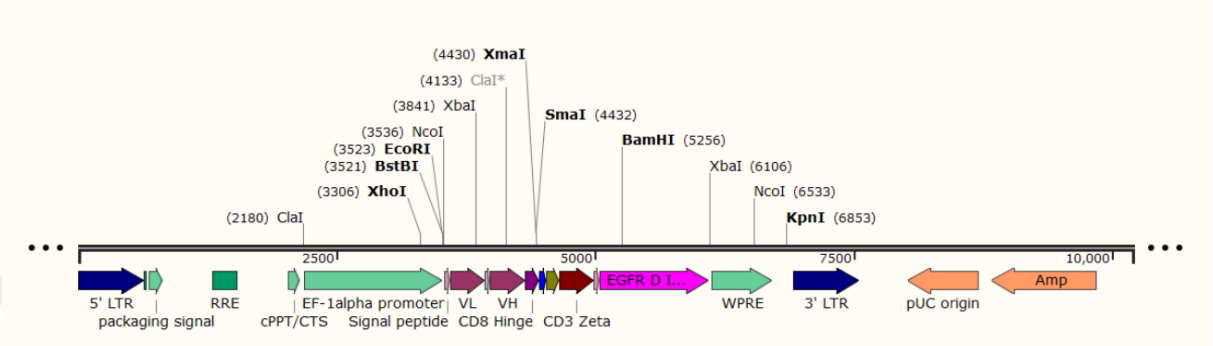

Figure 8: Designed plasmid construct.

3.2.2.2. Transformation, plasmid isolation

The plasmids were transferred to E. Coli Dh5a bacteria NEB® 5-alpha Competent E. coli (High Efficiency) by heat shock protocol as described previously. The bacteria were cultured in LB agar for 16-20 hours at 37°C and specific colonies were picked for mini and maxi cultures.

For plasmid isolation, the QIAfilter Plasmid Giga Kit (#12291, Qiagen) was used and the instructions of the kit were followed. The quantity and purity of the GD2 plasmid obtained as a result of isolation were measured with Nanodrop. DNA purity analysis was done by the gel electrophoresis method (Figure 9).

The quantity and quality of GD2 plasmids isolated after transformation were checked by Nanodrop (Table 4).

Table 4: Plasmid isolation results.

GD2 plasmid ng/µL	A260/A280	A260/A230
504.3	1.88	2.28

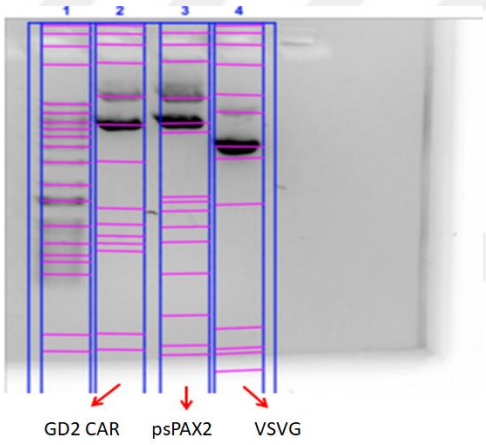

Figure 9: Plasmid gel electrophoresis.

3.2.2.3. Lentivirus production, titer determination

Plasmid isolation was done separately for GD2 CAR, envelope plasmid pCMV.VSVG, psPAX2 packaging plasmid. In the mass production of GD2 CAR lentivirus, 21 five-layer flasks were started. HEK293T cells were inoculated homogeneously in 100 ml of HEK complete medium DMEM (#11965084, Gibco) at $60x10^6$ cells per 5-fold flask. When the culture reached a confluency of 70-80% the flasks were discarded and 75 ml of OPTIMEM (#31985070, Gibco) containing 1%

penicillin-streptomycin (#03-031-5B, Biological Industries) was added and incubated at 37 °C for 1-2 hours before transfection. Fugene (#E2312, Promega) is used as a transfection reagent and GD2 CAR plasmid, pCMV.VSVG, psPAX2 plasmids were added to each layer of the five-layer flask. At the end of the serial culturing steps, the supernatants were removed and the pellets dissolved in 400 µl cold OPTIMEM (#31985070, Gibco) and aliquoted into cryovials as 1 ml and stored at -80 °C.

For determination of titration (Figure 10), Jurkat cells (#TIB-152, ATCC) were inoculated into a 96-well plate, 10,000 cells per well, in duplicate as the number of samples. Only 100µl of Jurkat's medium was added to a serial dilution part of the 96-well plate to titrate the virus in 6µl of the virus sample added into the first two wells of the serial dilution section, and 50µl transferred to the next wells (Figure 10). Titrated cells were incubated for 3 days in a 37 °C cell incubator. After 3 days of incubation, each well was mixed and 50µl was collected into glass tubes and 2µl anti-EGFR antibody (#352908, Biolegend) was added. It was incubated at +4 °C for 30 minutes. After incubation, 1ml DPBS was added to each sample and centrifuged at 1500rpm for 5 minutes. Supernatants were discarded, pellets were dissolved in 150µl DPBS (#02-023-1A, Biological Industries) and all concentrations were measured by flow cytometry (Cytoflex, Beckman Coulter).

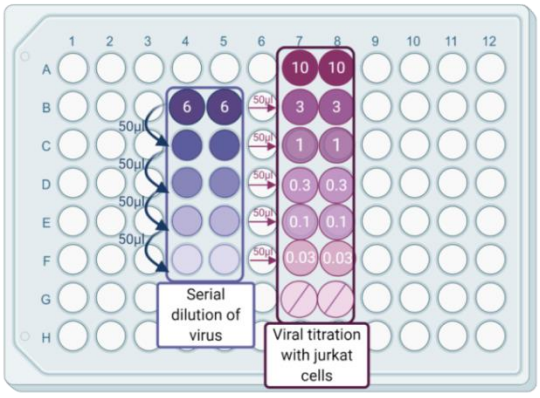

Figure 10: Experimental setup plan of the lentiviral titration experiment on Jurkat cells. (Created with BioRender.com)

3.2.3. PBMC isolation and GD2 CAR-M1 macrophage generation

3.2.3.1. PBMC isolation

With the appropriate method, 30 mL of peripheral blood (Ethics committee approval and consent form is attached in Appendix 2.) was taken into a citrate blood tube, and PBMCs were isolated by ficoll-plaque (#17-1440-02, Cytiva) gradient centrifugation. The tube was centrifuged at 21˚C at 800G for 25 minutes. The PBMCs were pipetted out and transferred to new 50 ml falcon tubes. DPBS (Without ca, mg) (02-023-1A, Biological Industries) was added to the collected cell suspension and was centrifuged at 21˚C and 400G for 10 minutes. After centrifugation, the supernatant was discarded; the pellet was diluted with complete DMEM medium DMEM (#11965084, Gibco).

3.2.3.2. M1 macrophage generation

For the selection of CD14 positive cells from the PBMC cell group, the magnetic selection was performed using CD14 magnetic beads (#130-050-201, Miltenyi), following the manufacturer's protocol. Selected CD14+ cells were centrifuged at 21˚C and 400G for 10 minutes to and the pellet was dissolved in 1.5 ml of macrophage/monocyte / DC medium. It was planted in a 24 well plate and incubated in a 37°C cell incubator for 10 days. Fresh medium was added every 5 days.

Table 5: Specific differentiation culture conditions.

Cell type	Medium content
Monocyte	• DMEM high glucose (#11965084, Gibco) • 10% FBS (#10500064, Gibco) • 1% Penicillin-Streptomycin (#03-031-5B, Biological Industries)
M1 macrophage	• DMEM high glucose (#11965084, Gibco) • 10% FBS (#10500064, Gibco) • 1% Penicillin-Streptomycin (#03-031-5B, Biological Industries) • GM-CSF (50µg) (#P04141, CellGenix) • IFN- γ (100µg) (#285-GMP-100, R and D systems)
Dendritic cell	• DMEM high glucose (#11965084, Gibco) • 10% FBS (#10500064, Gibco) • 1% Penicillin-Streptomycin (#03-031-5B, Biological Industries) • GMC-SF (50µg) (#P04141, CellGenix) • IL-4 (250µg) (#130-094-117, Miltenyi)

Flow cytometric analysis (Cytoflex, Beckman Coulter) was performed to determine macrophage-specific antigens by observing fully differentiated M1 macrophages on the 10th day and to confirm that the formed cell group was M1 macrophage, and dendritic cells were compared with monocytes. Antibodies CD206-FITC (#130-123-671, Miltenyi), CD163-vioblue (#130-112-134, Miltenyi), CD14-PE (#130-110-519, Miltenyi), CD86- Pevio. 770 (#130-113-573, Miltenyi) were used.

3.2.3.3. Transduction

After cell differentiation was observed under the microscope, 5MOI GD2 CAR LV was combined with vectofusin-1(# 130-111-163, Miltenyi) and centrifuged for 1 hr 400G 4 °C. Medium changed after 24 hr. Following the culturing steps the CAR

Macrophage and control macrophage wells trypsinized and analyzed by macrophage flow panel and CAR expression by flowcytometry.

3.2.4. BE(2) neuroblastoma cell line mcherry labeling

BE(2)C cells line (#CRL-2268, ATCC) were prepared for labeling when cell viability and number of neuroblastoma reached an optimal level. 100,000 cells were planted in 5 wells of 24 well plates in 500 µl medium. 5 MOI of fluc mCherry lentivirus was placed on the cells. It was placed in the incubator at 37 °C. After 24 hours, 1 ml medium is added to the wells. It was placed in the incubator at 37°C. After 48 hours, the cells were removed by trypsinizing (#03-053-1B, Biological Industries) and the cell number was taken and planted in 3 ml of 6 well plates in 2 wells. After 3 days, the cells were removed by trypsinizing, the number of cells was taken and the T25 plate was transferred. 100 µl of the sample was taken for flow reading.

3.2.5. Transduction of effector cell lines

NK-92 (#CRL-2407, ATCC), Hassasin, and U937 cell lines (#CRL-1593.2, ATCC) were prepared for transfection when cell viability and number of cells reached an optimal level. 200,000 cells were planted in 12 wells of 24 well plates in 1 ml medium. 5 MOI of GD2 lentivirus was placed on the cells. The plate was placed in the incubator at 37 °C. After 6 hours, all wells are combined and centrifuged at 180G 10 min. Supernatant discarded and pellet dissolved with fresh medium. Cells are plated at 1 well of 6 well plate. It was placed in the incubator at 37 °C. After 2 days, the cells were transferred to the T25 plate was. On the fifth day of transfection, 100 µl of the sample was taken for anti-EGFR antibody (#352908, Biolegend) flow reading that was made to determine the ratio of CAR-expressing cells for hassasin an

NK-92. For U937 cell 100 µl of the sample was taken for Human TruStain FcX (#422301, Biolegend) and Human IgG, F(ab')2 Fragment specific Antibody (#MOB-0239MC, Creative Biolabs) staining protocol than flow reading that was made to determine the ratio of CAR-expressing cells.

The magnetic selection method was applied for GD2 CAR NK-92 and GD2 CAR hassasin to increase the percentage of CAR-positive cells. CAR positive cells were selected using Human EGFR Biotinylated antibody (#FAB9577B-100, R and D Systems) and Streptavidin Microbeads (#130-048-101, Miltenyi) according to the manufacturer's protocol.

3.2.6. Efficacy tests

It was ensured that the cells to be tested for efficacy and the target tumor cell BE(2)C had high cell viability. 25 thousand BE(2)C (mcherry labeled) were seeded in 500 µl onto 24 well plates. Then, effector cell groups were seeded on tumor cells in 500 microliters with an effector: target ratio of 1:1, 5:1, 10:1. In the experiments where the efficacy was tested in the presence of PBMC, 25 thousand PBMC cells were added in 100 microliters by CTV (Cell trace violet) (#C34557, Invitrogen) marking into the same experimental group. CTV labeling was performed according to the manufacturer's protocol and it was confirmed that the cell population with CTV was above 95% before starting the experiment. In the efficacy tests established by irradiation, cells were taken into cryo bags in ringer lactate (#PPB-2001252, Polypharma) containing 1% HSA (human serum albumin) (#Octapharma CSL Behring) and taken to Acıbadem Altunizade hospital to be irradiated at 1000 Gy. At the end of the irradiation, the cells were immediately brought to the laboratory, washed 2 times with DPBS, and the experimental setup was started by taking the cell number.

3.2.6.1. Flow cytometry

At the end of the 48th hour, the cells were removed in the activity test, and flow cytometric analysis was performed by staining with CD56-PE (#981202, Biolegend), CD107a-PerCp.cy5.5(#328616, Biolegend), CD4-APC.cy7 (#317418, Biolegend), CD8-FITC (#301050, Biolegend), CD25-APC (#302610, Biolegend) antibodies. Cells were categorized by opening mCherry (BE(2)C), CTV (PBMC) channels.

3.2.6.2. Cytokine bead array

The cytokine panel was tested by collecting the supernatant in the efficacy experiments after 48 hr. For this, the MACSPlex Cytokine Bead Array kit (#130-099-169, Miltenyi) was used and the manufacturer's protocol was followed (Figure 11). Again, the manufacturer's protocol was followed and the standard beads were studied by serial dilution and the standard curve was derived for each cytokine. Experimental values were analyzed and interpreted on this standard curve.

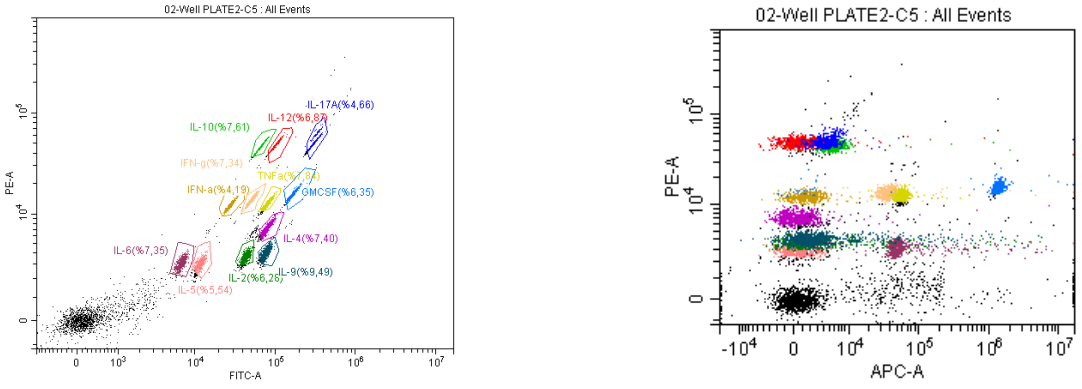

Figure 11: The location of each bead in the flow plane as a result of the Cytokine Bead Array.

3.2.6.3. Rozette test and wright eosin staining

GD2 CAR U937/U937 and BE(2)C cells were mixed at a glass tube for 1:4 effector: target ratio at 500 µl total. After 5min. incubation at 37°C, cells were centrifuge at 100G for 5 min. After centrifugation cells were incubated at 4°C for 1 hour. 10 µl cell mixture dropped on top of the glass slide and the drop was allowed to dry for 15 minutes. After the drop dried, 2 ml of Wright's eosin methylene blue solution (#101383, Merck) was added to cover it and waited for 15 minutes. At the end of 15 minutes, 1 ml of distilled water was added and incubated for another 5 minutes. The slide is carefully rinsed under running water to allow excess paint to drain. After waiting half an hour for the slides to dry, the rosette formations were observed and scored under the light microscope.

3.2.6.4. MTT assay

MSC collected according to the collection procedure and counted. 96 well plates were used. Cell concentration has been set to in every 100 µl, 10000 cells. 100 µl loaded every well of 96 well plates. After 24 hours 20x106 U937 and GD2 CAR U937 cells collected and performed lysate preparation protocol. 20 million cells were reduced to 4 ml volume and taken into cryovials. During 1-2 min, it was thrown into liquid nitrogen. Frozen cells were thawed at 37°C and vortexed, this process was repeated three times. Cells were centrifuged at 400g for 10 minutes. Samples were prepared as 20%, 10% 1% cell lysates in MSC NutriStem® XF Medium (#05-200-1A, Biological Industries). 0% sample was prepared as a complete MSC medium. 100 µl of the prepared samples were added to the MSC and cultured for 72 hr. 100 µl of the solution was withdrawn from each well. 100 µl of MTT solution (#CT01, MercMillipore) was added and incubated for 4 hours at 37°C. MTT solubilized with 100 µl isopropanol (#A3928, PanReac Appli chem). The plate was shaken for 10 minutes in the dark area. The plate was read at 570 nm in the Omega Elisa reader.

3.2.7. Quality control tests

Mycoplasma, endotoxin, VDRL (Venereal Disease Research Laboratory), fungus, aerobic-anaerobic bacteria culture, Hepatitis B, Hepatitis C, Human Immunodeficiency Virus (HIV), Epstein-Barr virus (EBV) virus control tests were performed by Acıbadem Labmed Laboratory.

3.2.8. TEM

As previously described, TEM analyzes were performed by Acıbadem University, Department of Histology and Embryology (53).

3.2.9. Statistical analysis

Normally distributed data in graphs was analyzed using student's t-tests for two independent means. Graphs report the mean and standard deviation of the mean. The threshold of significance for all tests was set at * $p<0.05$. NS represent Non-Significant. Statistical analyzes were performed on GraphPad Prism version 8.4.3.

4. RESULTS

4.1. GD2 Lentivirus Titration and Safety

The concentration corresponding to the range of 5% to 10% of CAR expression after viral titration was measured by flow cytometry and taken as a basis (0.03). IFU/mL of the virus was calculated according to this concentration and 21.5 x10^6 IFU/mL was found (Figure 12).

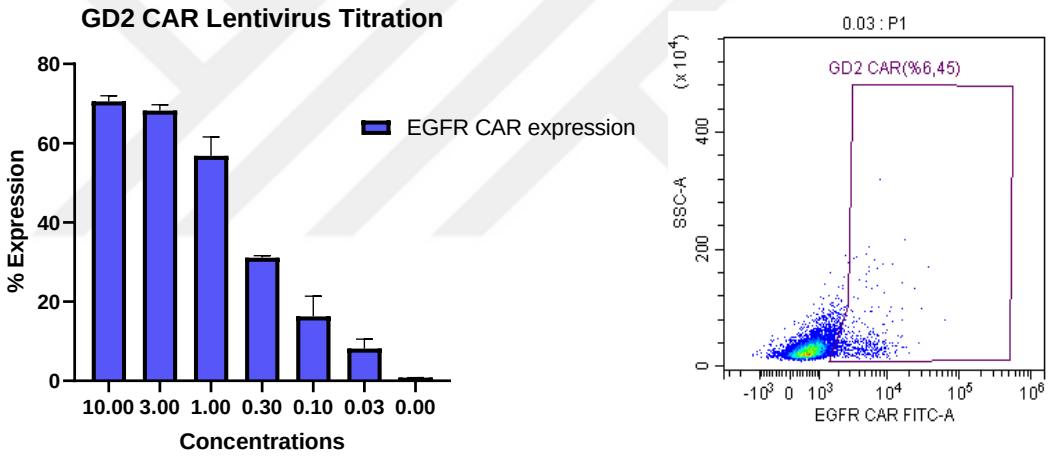

Figure 12: GD2 CAR Lentivirus titration assay flow result.

No viral particles were found in the RCL test, which was established to prove the virus's safety and non-replicative competence (Figure 13).

A.

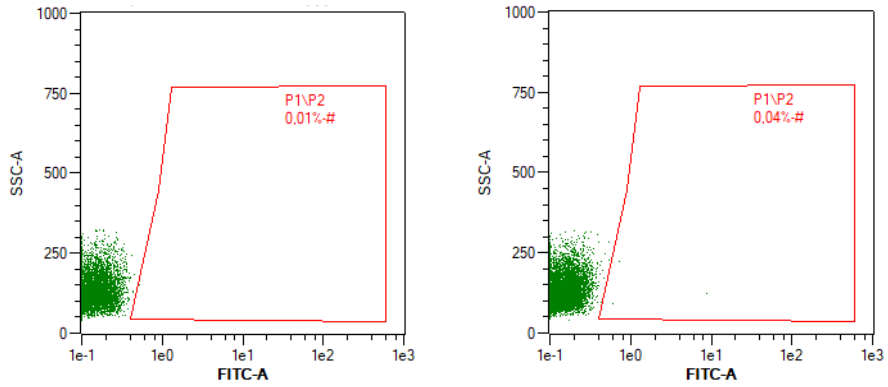

B.

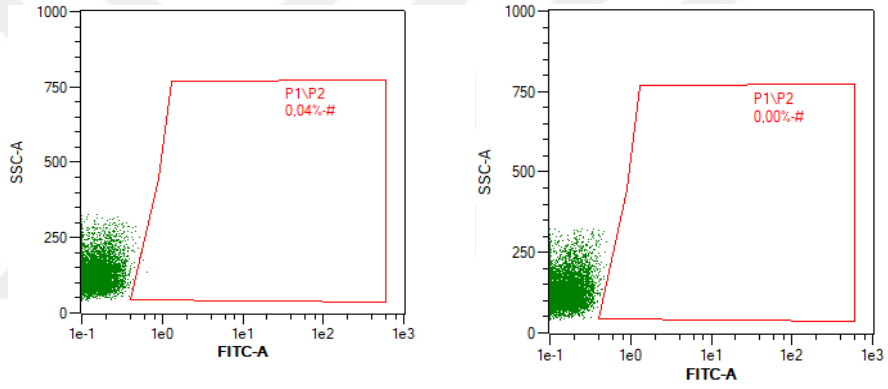

Figure 13: RCL test of GD2 CAR lentivirus. A. Viral residue in culture made from the supernatant of 30µl GD2 CAR lentivirus-infected cells. B. Viral residue in culture made from the supernatant of 10 µl GD2 CAR lentivirus-infected cells. Duplicate samples were presented.

4.2. BE(2)C Neuroblastoma Target Cell-Line Labeling

The flow results of the BE(2)C neuroblastoma cell line transduced with mCherry lentivirus proved the transduction efficiency to be over 99.39% at the first measurement and 96.50% one month after (Figure 14). The mCherry expression of BE(2)C cell lines was confirmed also by fluorescent microscopy (Figure 15).

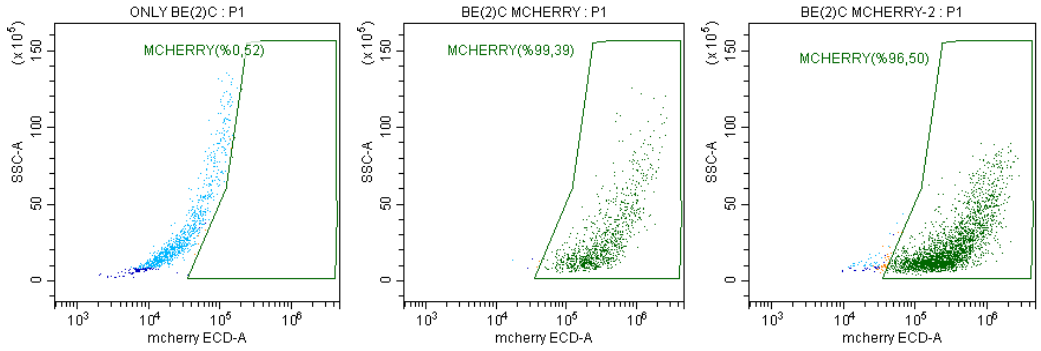

Figure 14: BE(2)C target cell line mCherry labeling.

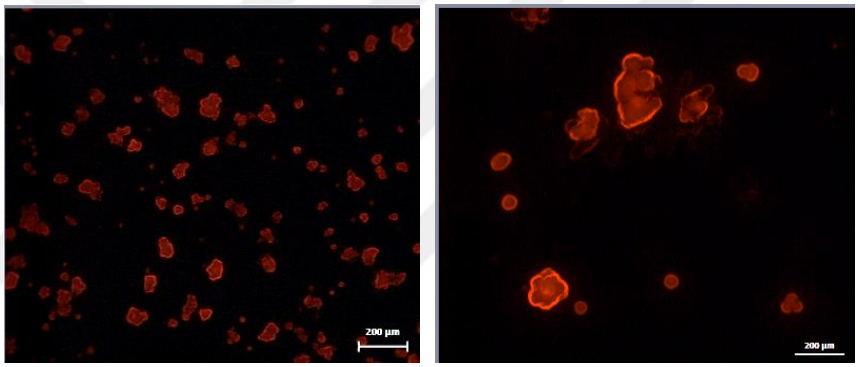

Figure 15: Fluorescent microscopy image of BE(2)C mCherry expression under 40X and 100X magnification.

4.3. Results of GD2 CAR in M1 Macrophage

Flow cytometric analysis was performed to determine macrophage-specific antigens by observing fully differentiated M1 macrophages on the 10th day and to confirm that the formed cell group was M1 macrophage. We have also compared the dendritic cells with monocytes. Increased CD206, CD163, and CD86 expressions prove that the cells formed are M1 macrophages (Figure 16).

The cells were also checked under light microscopy on day 10 and we observed that the cell morphological features were presenting fully differentiated M1 macrophages (Figure 17).

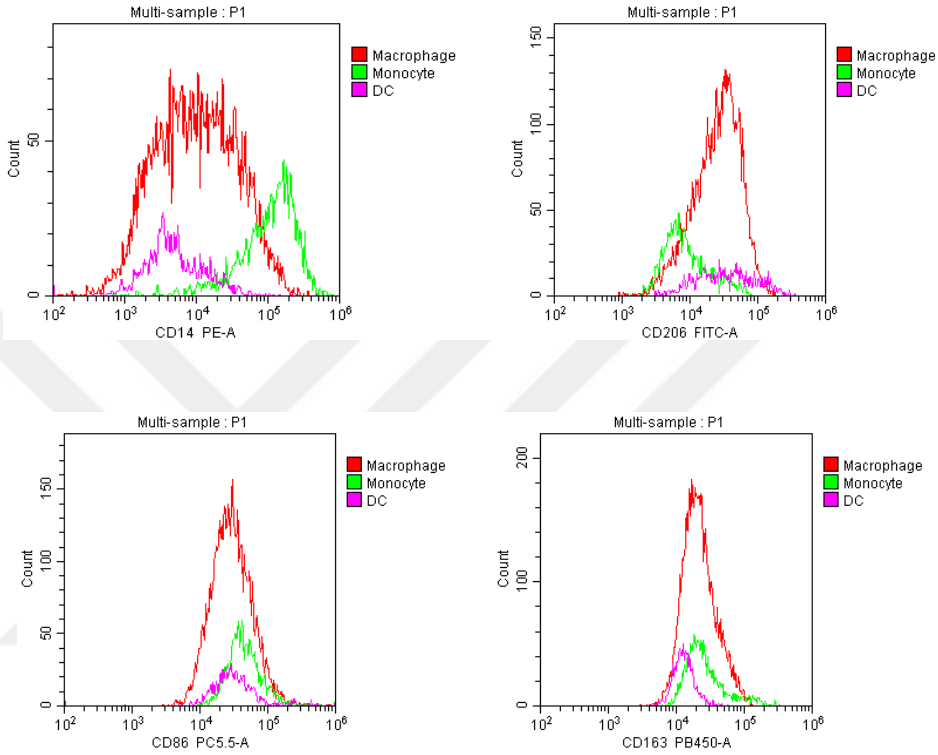

Figure 16: Macrophage flow panel. Comparison of CD14, CD206, CD86, and CD163 expression levels of cell groups, respectively.

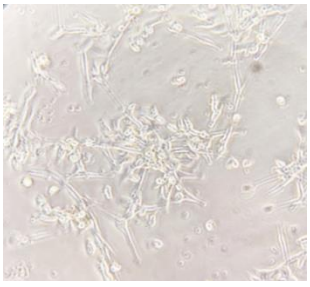

Figure 17: M1 macrophage morphology. The image was obtained with 40X magnification.

The macrophages naturally express EGFR. Hence, the transduction efficiency of macrophages with GD2 CAR lentivirus was determined by Fab antibody staining. We found that 29% of macrophages were expressing GD2 CAR (Figure 14).

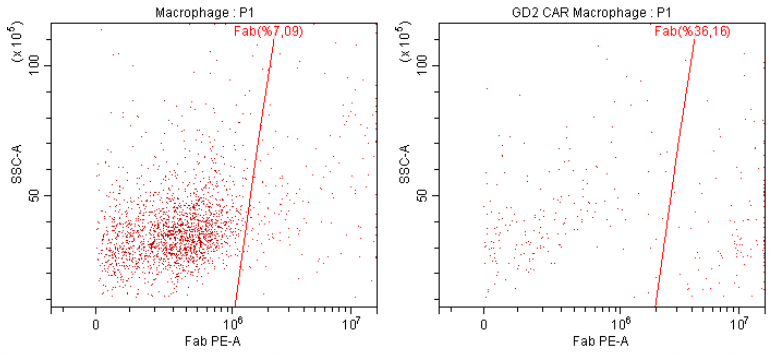

Figure 18: GD2 CAR expression of macrophages. The CAR expression rate was normalized by subtracting the percent Fab positivity of untransduced macrophages from the percent of transduced ones.

We have checked the mCherry expression of surviving BE(2)C cells after 24 and 48 hours incubation of macrophage and CAR macrophage on BE(2)C at different E: T (Efecttor: target) ratios. The superiority of CAR macrophage over macrophage in tumor killing, especially after 48 hours, was concentration-dependent (Figure 19.A**)** and the difference was significant.

Also, we have determined the percentage of BE(2)C neuroblastoma tumor cells that survive in the medium after incubation of CAR macrophage and macrophage with tumor cells for 48 hours. Both groups have a superior killing power compared to the only tumor group, however, increased tumor-killing activity is observed in CAR macrophages (Figure 19.B). Moreover, the antitumoral capacity of macrophage and GD2 CAR macrophage were measured, and after 48 hours of incubation of CAR macrophage and BE(2)C tumor cell together, it was proven that the mcherry expression was reduced (Figure 20).

A.

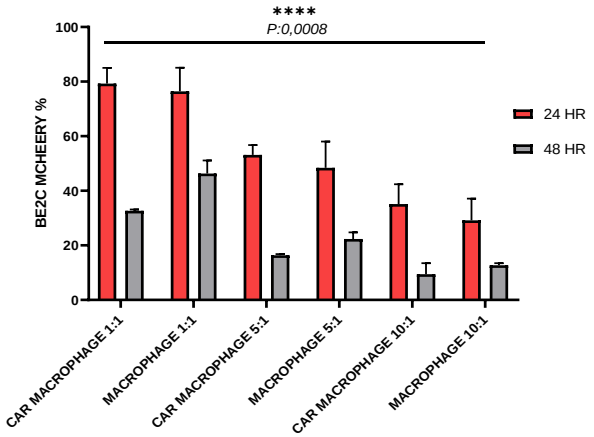

B.

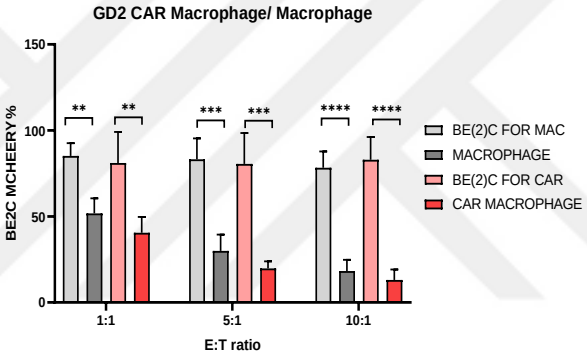

Figure 19: CAR macrophage efficacy analysis by flow cytometry. A. Tumor killing capacity of CAR macrophage and car macrophage for two days. B. Tumor-killing capacities of CAR macrophage and macrophage at 48 hours compared to tumor only group. Experimental studies were repeated in duplicate at three different times. The differences between the two groups were calculated by the Student-t-test, $p<0.005$.

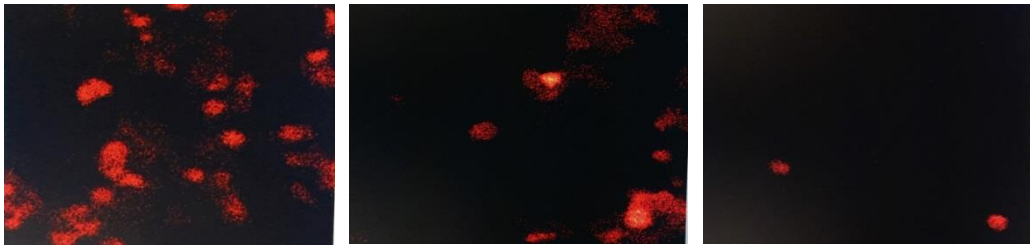

Only BE(2)C | Macrophage+BE(2)C | GD2 CAR Macrophage +BE(2)C

Figure 20: Confocal microscope representation of tumor-killing capacity**.** After 48 hours of incubation, mCherry reflection of experiment groups with 10:1 effector: target ratio was visualized under a confocal microscope with 20X magnification.

Cytokine bead array (CBA) assay was used to measures the cytokines formed in the medium after 48 hours of incubation of CAR macrophage and macrophage with tumor cells. We have calculated Th1/Th2 ratio and we detected an increased Th1 reaction in CAR macrophage groups but the result was not statistically significant (Figure 21).

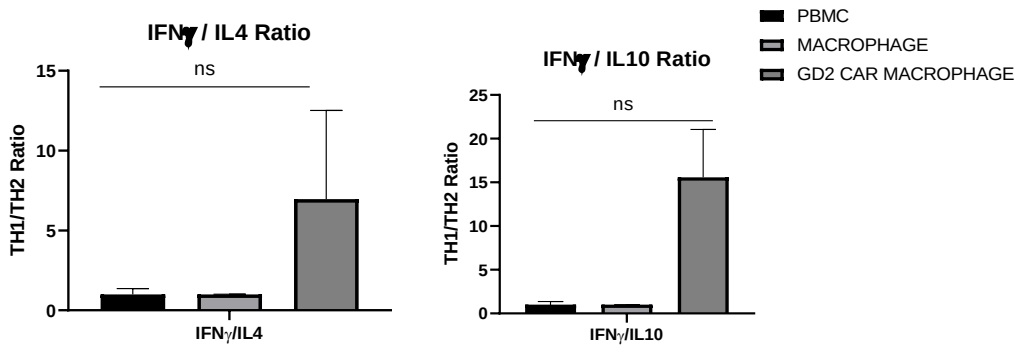

Figure 21: TH1 cytokine response of GD2 CAR macrophage. Student-t test was used as statistical analysis, $p<0.005$.

4.4. Results of GD2 CAR in NK-92 and Hassasin Cell-Line

We measured the CAR expression at the end of day 5 of NK-92 and Hassasin cells transduced with GD2 CAR lentivirus by flow cytometry. The day 5 expression was found to be between 20-30%. Following the EGFR magnetic selection of transgenic cells expressing CAR, the expression levels were increased to 96% and 93% respectively (Figure 22).

A.

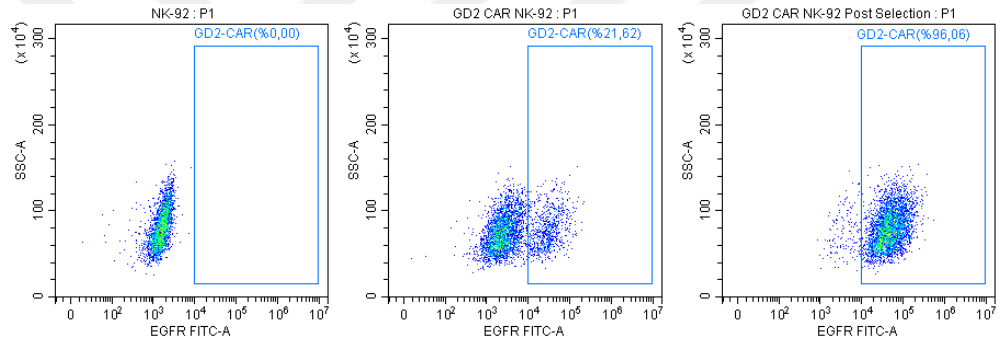

B.

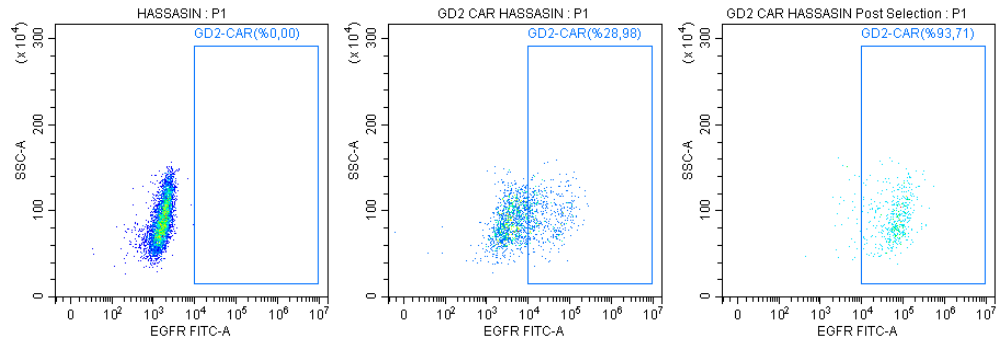

Figure 22: GD2 CAR expression of NK-92 and Hassasin cells. A. GD2 CAR expression result before and after selection compared to non-transduced NK-92 cells. B. GD2 CAR expression result before and after selection compared to non-transduced Hassasin cell.

To use the cell line in clinical applications, 1000 Gy irradiation was performed and the tumor-killing capacity of the cells at 24 and 48 hours was examined. Despite the irradiation, the cells retain their anti-tumoral capacity both for NK-92 and Hassasin cell lines (Figure 23 and Figure 24 respectively).

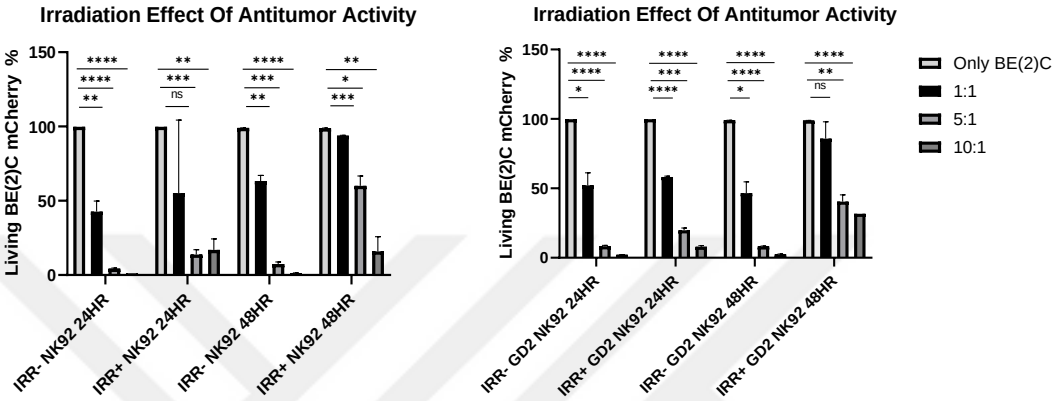

Figure 23: Irradiation effect on NK-92 and GD2 CAR NK-92.

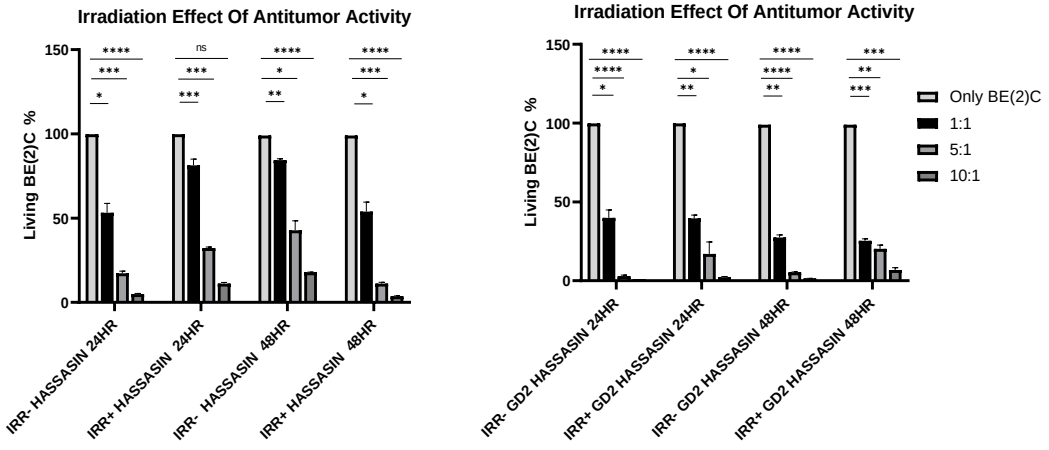

Figure 24: Irradiation effect on Hassasin and GD2 CAR Hassasin. Experimental studies were repeated in duplicate at three different times. Student-t test was used as statistical analysis, $p<0.005$.

We have compared the tumor-killing capacity of irradiated GD2 NK-92 cells and GD2 Hassasin cells at 24 and 48 hours. Although both groups still preserved their antitumor capacity after 48 hours, the efficacy of the GD2 Hassasin was higher (Figure 25).

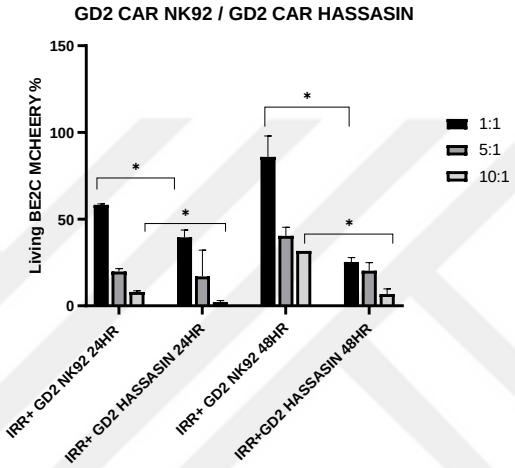

Figure 25: Antitumor efficacy comparison of irradiated GD2 NK-92 and GD2 CAR Hassasin cells**.** Experimental studies were repeated in duplicate at three different times. Student-t test was used as statistical analysis, $p<0.005$.

After irradiation, effector cell groups were incubated with BE(2)C tumor cells at different concentrations, keeping the same experimental standards. When tumor cell populations in the medium were compared at the 48th hour of incubation, it was shown that the most effective group in terms of tumor-killing capacity was the GD2 CAR Hassasin group (Figure 26A). When PBMCs were added to the medium with the same experimental groups at the same amount, there was no increase in their tumor-killing capacity (Figure 26B).

A.

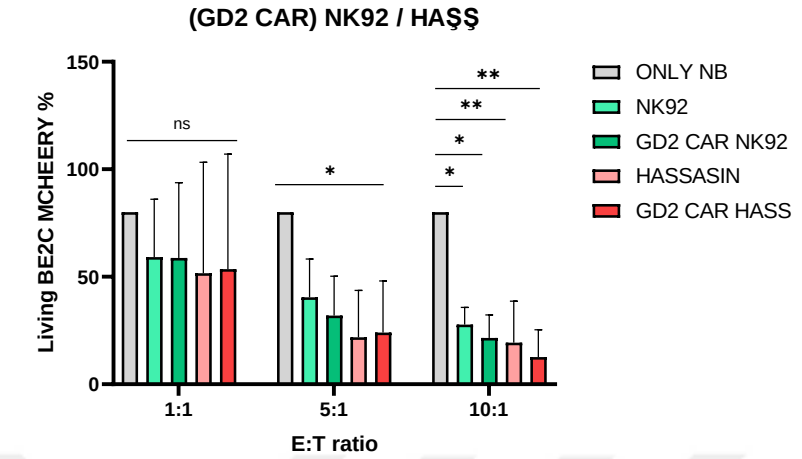

B.

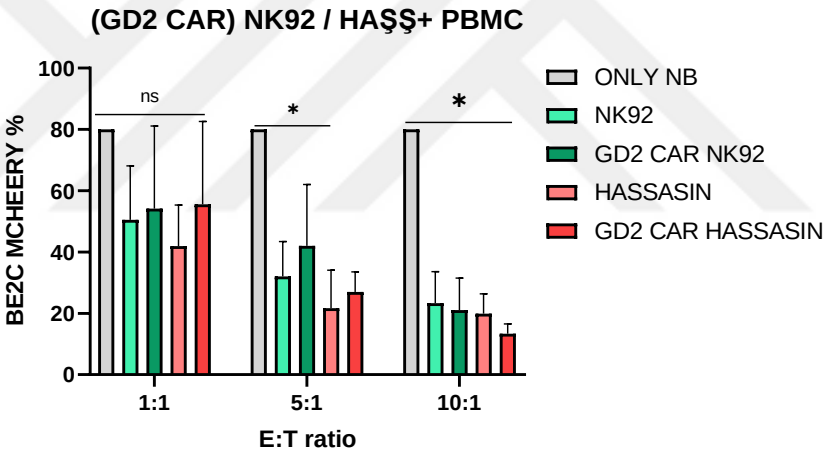

Figure 26: GD2 CAR NK-92 and GD2 CAR Hassasin efficacy tests. Experimental studies were repeated in duplicate at three different times. E: T represents Effector: Target. Student-t test was used as statistical analysis, $p<0.005$.

The CBA test showed significantly increased TH1 response in the medium when PBMCs were present (Figure 27). The TH1 anti-tumorigenic cytokine response was mostly seen in the GD2 CAR Hassasin group.

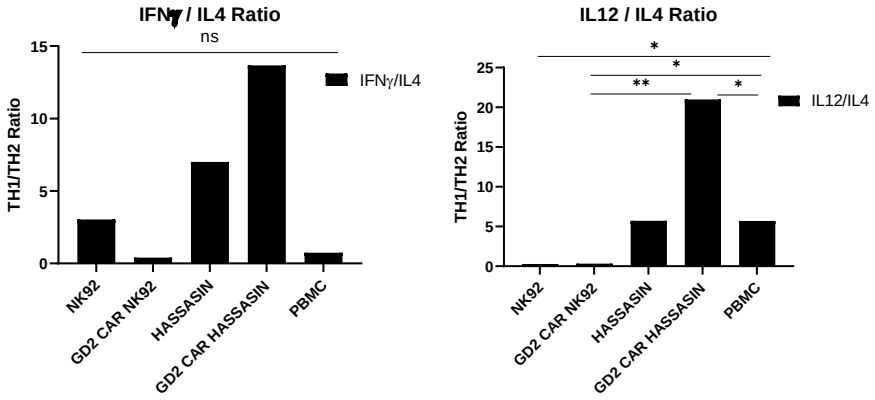

Figure 27: TH1 cytokine response of GD2 CAR NK-92 and GD2 CAR Hassasin. Experimental studies were repeated in duplicate at three different times. Student-t test was used as statistical analysis, $p<0.005$.

In addition to these data, the activated (CD25+) CD4 and CD8 ratios were analyzed by flow cytometric analysis to better understand the T cell response on the same experimental groups. In direct proportion to the increasing concentration, it was determined that the most effective group in stimulating T cells was GD2 CAR Hassasin (Figure 28).

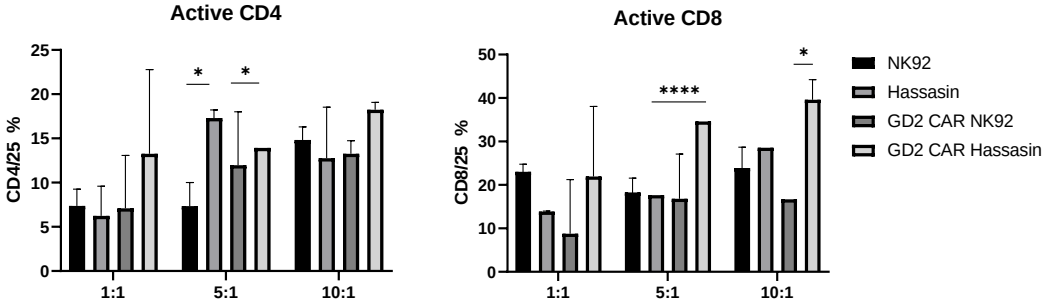

Figure 28: T cell activation response**.** Experimental studies were repeated in duplicate at three different times. Student-t test was used as statistical analysis, $p<0.005$.

It was also confirmed by CBA analysis that the sensitized cell line secretes IL-12.

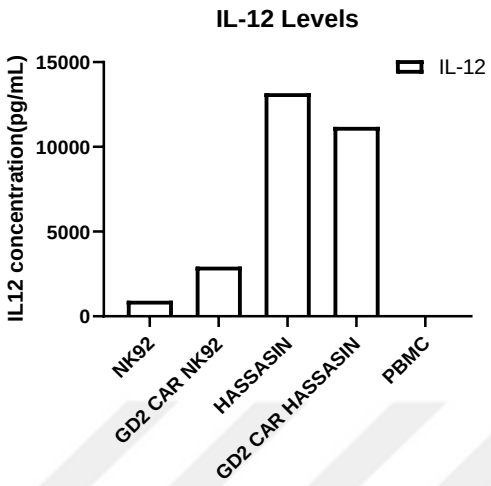

Figure 29: IL-12 cytokine secretion of Hassasin cells.

We have checked the duration of the efficiency of the Hassasin cell lines and showed that the generated transgenic cell line still maintains its expression in the second month after generation (Figure 30).

A.

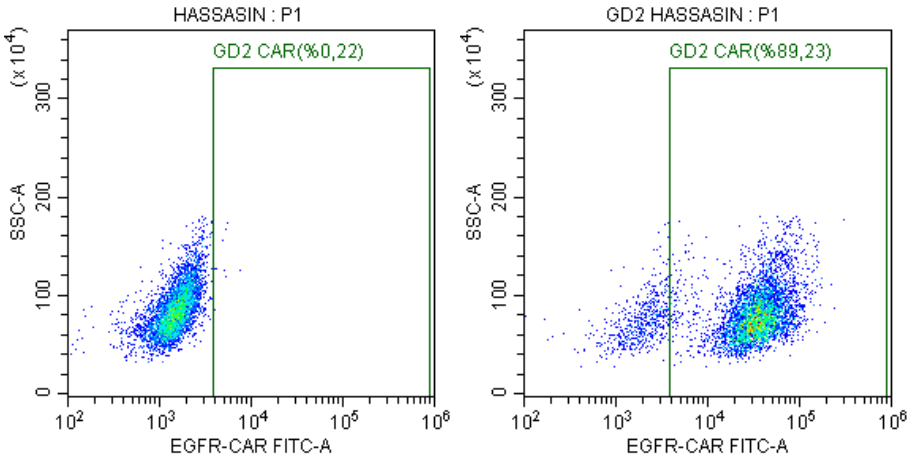

B.

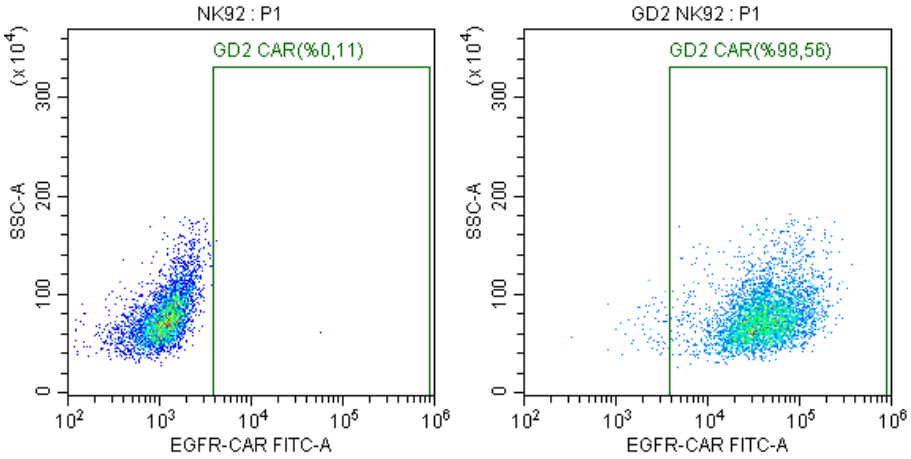

Figure 30: GD2 CAR expression after 2 months. A. GD2 CAR expression after 2 months compared to non-transduced Hassasin cells. B. GD2 CAR expression after 2 months compared to non-transduced NK-92 cell.

Table 6: Quality control analyses of GD2 CAR NK-92 and GD CAR Hassasin.

Test	Method	Reference interval	Result
Endotoxin	Gel clot (LAL)	+/-	Negative
Mycoplasma	DNA PCR	+/-	Negative
Fungus	TSA plaque assay	+/-	Negative

4.5. Results of GD2 CAR in U937 Cell-Line

U937 cells naturally express EGFR so we determined the GD2 CAR lentivirus by Fab antibody staining and showed that 51% of U937 cells were expressing GD2 CAR (Figure 31).

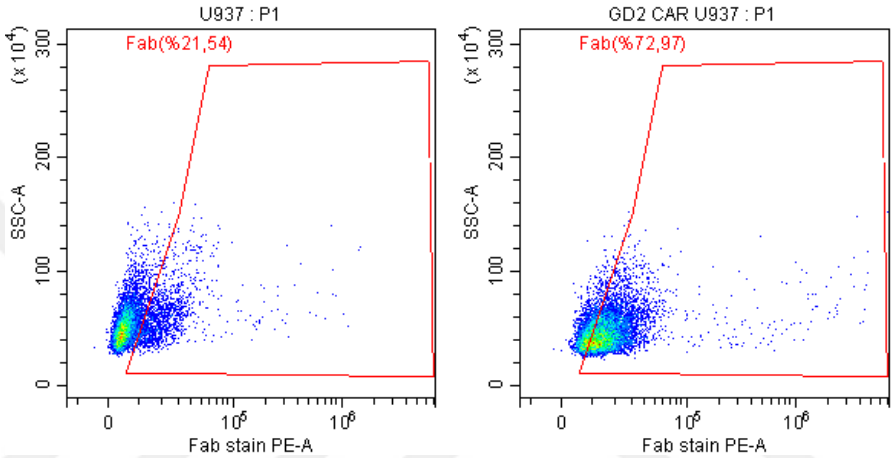

Figure 31: GD2 CAR expression of U937 cells.

Rosette formations of GD2 CAR U937 and U937 cells with BE(2)C tumor cells counted under light microscopy (Figure 28). When the numbers of U937 forming and not forming rosettes were compared, a 40% rosette formation increase was found in the GD2 CAR U937 group due to the CAR construct. After engineering the CAR construct, naive U937 cells attach to tumor cells with an increase of 40% (Table 7).

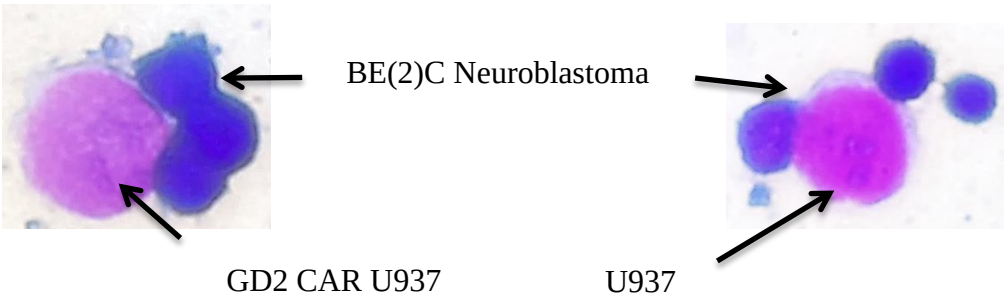

Figure 32: Rosette formation by GD2 CAR U937 and U937 cells with BE(2)C tumor cells**.** Cells adhering to more than 2 tumor cells at the same time were considered to form rosettes. Cells were examined at 100X magnification under a light microscope colored with eosin staining.

Table 7: Rosette observations.

	Total number of U937 cells counted	**Number of U937 that do not form rosettes**	**Number of rosette formed**	**Estimated CAR percentage**
U937	49	33	16	%32
GD2 CAR U937	52	16	36	%70

The tumor-killing capacity of the U937 cells at 24 and 48 hours was examined after 1000 Gy irradiation and found that the cells retain their anti-tumoral capacity despite irradiation (Figure 33) and the difference was significant between effector groups and only BE(2)C.

A.

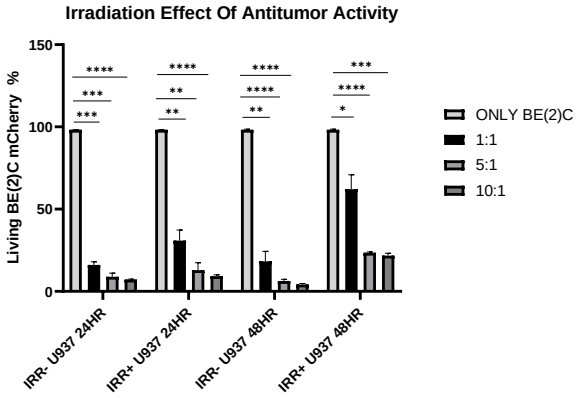

B.

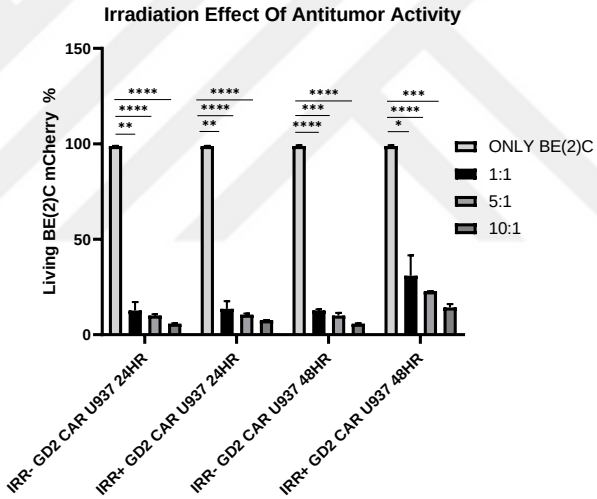

Figure 33: Irradiation effect on U937 and GD2 CAR U937 cells. A. Tumor-killing capacity of irradiated and non-irradiated U937 cells for 24 hours and 48 hours. B.Tumor-killing capacity of irradiated and non-irradiated GD2 CAR U937 cells for 24 hours and 48 hours. Experimental studies were repeated in duplicate at three different times. Student-t test was used as statistical analysis, $p<0.005$.

After irradiation, effector cell groups were incubated with BE(2)C tumor cells at different concentrations, keeping the same experimental standards. When tumor cell populations living in the medium were compared at the 48th hour of incubation, it

was shown that the most effective group in terms of tumor-killing capacity was the GD2 CAR U937 (Figure 34A). When PBMCs were added to the medium with the same experimental groups at the same amount, there was no increase in their tumor-killing capacity (Figure 34B), whereas an increased TH1 response occurred in the medium in the presence of PBMCs (Figure 35**)** and the TH1 anti-tumorigenic cytokine response was mostly seen in the GD2 CAR U937 group. In addition to these data, (CD25+) CD8 activation, granulation (CD107a+), and PBMC proliferation were enhanced with GD2 CAR U937 (Figure 36).

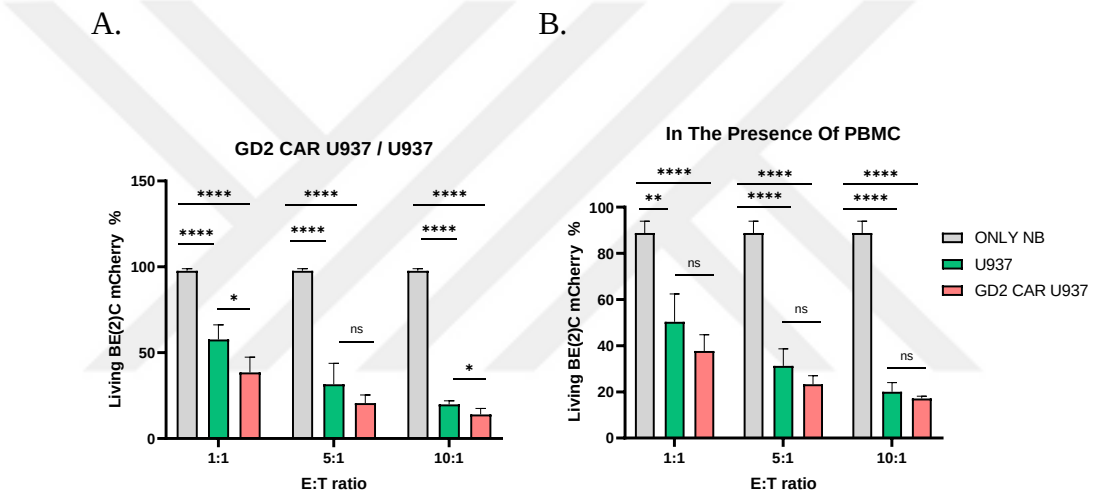

Figure 34: Tumor-killing efficacy of GD2 CAR U937 cells. E: T represents Effector: Target

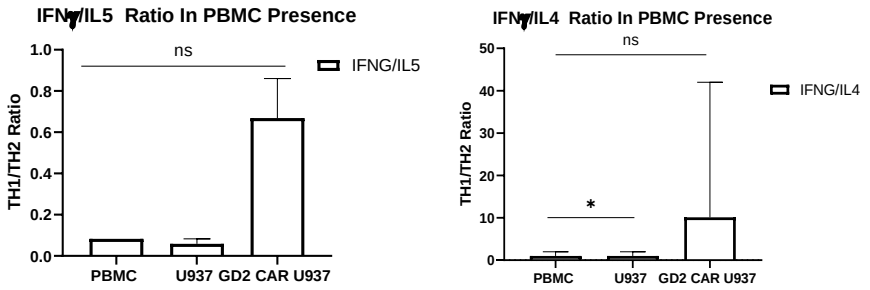

Figure 35: TH1 cytokine response of GD2 CAR U927 cells.

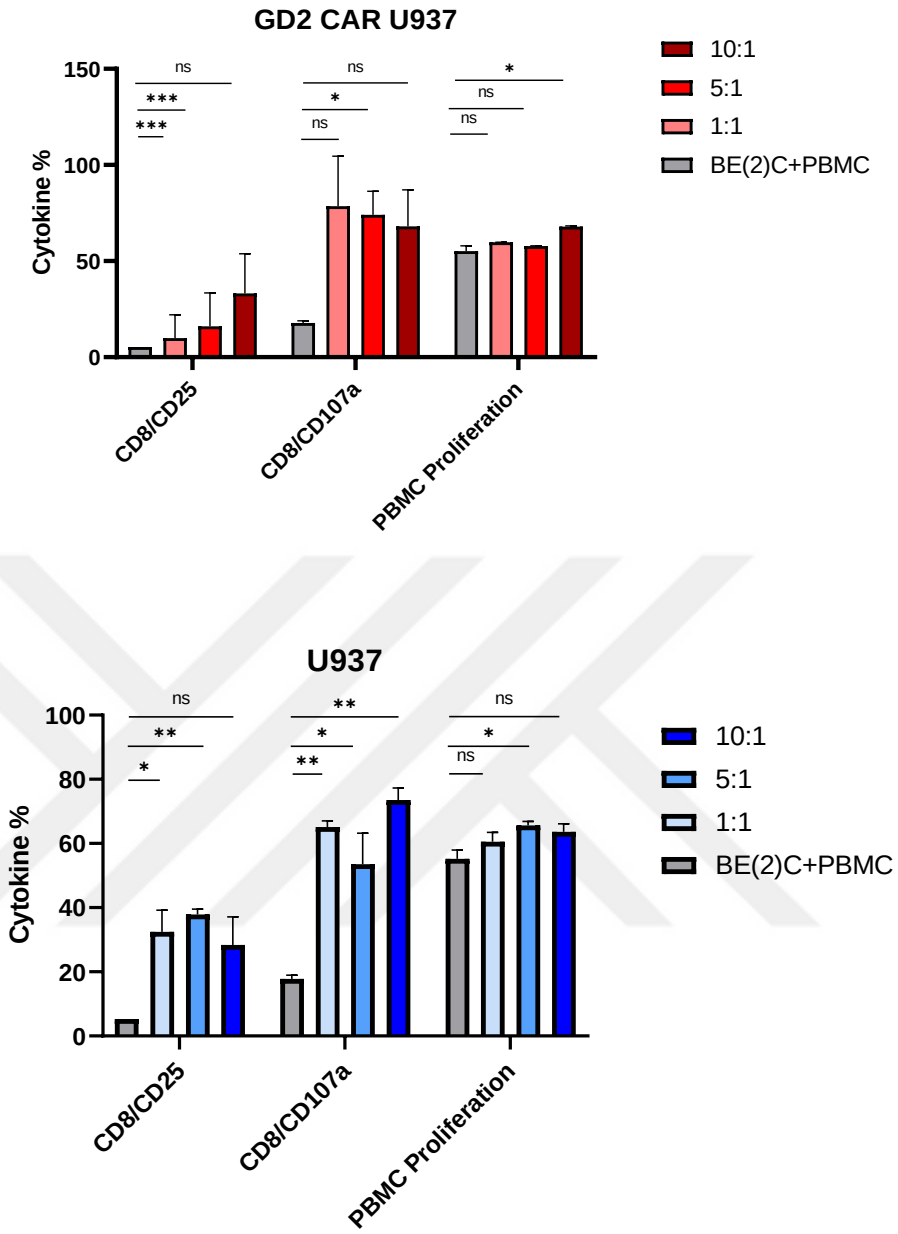

Figure 36: PBMC activation OF GD2 CAR U937 cells.

We performed quality-control tests and showed that the produced GD2-U937 cells are sterile and suitable for clinical application (Table 8)

Table 8: Quality control analyses of GD2 U937.

Test	Method	Reference interval	Result
VDRL	Card Test	+/-	Negative
Hepatitis B Virus (HBV)	DNA QRT- PCR	1,4-7,3 log IU/mL 1 log IU/mL	Negative
Hepatitis C Virus (HCV)	RNA QRT- PCR	1,5-7,2 log IU/Ml 1,3 log IU/mL	Negative
Human Immunodeficiency Virus (HIV)	RNA QRT- PCR	2-8 log/Ml 1,88 log IU/mL	Negative
Endotoxin	Gel clot (LAL)	+/-	Negative
Mycoplasma	DNA PCR	+/-	Negative
Fungus	TSA plaque assay	+/-	Negative
Aerobic-anaerobic bacteria	Bactec	+/-	Negative

After irradiation, the number and viability of GD2 CAR U937 cells were monitored for eight days. The amount of decrease in viability and cell number, in the following days shows that cells can remain alive in in vitro for a week (Figure 37). Thereupon, after combining with the tumor, the killing capacity of these cells was measured every day after irradiation, and the effect of irradiation on antitumoral capacity was demonstrated. At the end of the day 4, the GD2 CAR U937 cells had no killing capacity (Figure 38).

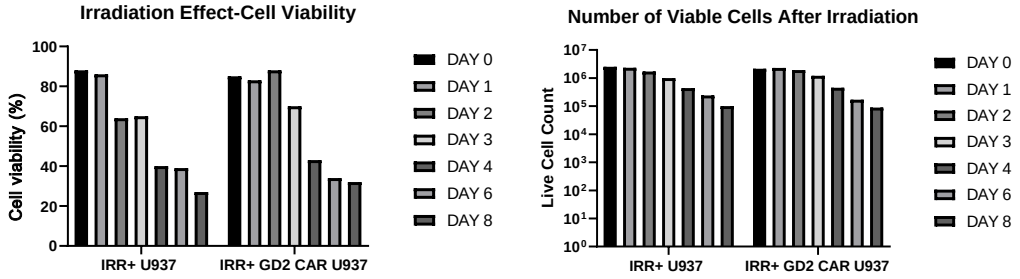

Figure 37: Daily cell count and viability of irradiated GD2 CAR U937 and U937 cells.

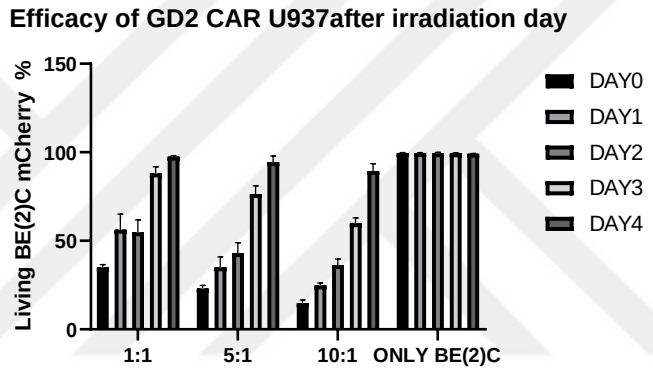

Figure 38: 24-hour activity tests set up every day after irradiation.

In the MTT experiment performed after incubation of umbilical cord-driven MSC cells and GD2/U937 cell lysates, no decrease was detected in MSC viability, which shows that the GD2 U937 cells did not have a cytopathic and toxic effect on healthy cells (Figure 39). No viral particles were encountered after TEM analysis of U937 and GD2 CAR U937 (Figure 40). This supports the safety of the GD2 CAR U937 cell line developed with the lentiviral vector. In the supplementary data in Appendix 3, following the inoculation of U937 and GD2 CAR U937 in lysate form on MSC at 10% concentration, the presence of cytopathic effects in MSC cells was followed for 7 days with a light microscope. The absence of any change in MSC morphology once again proved the safety of GD2 CAR U937 cells on somatic cells.

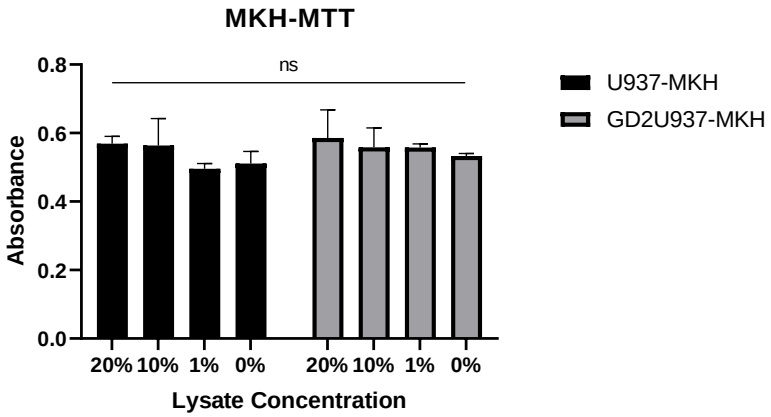

Figure 39: Assay of cytopathic effect on MSC of GD2 CAR U937 cells with MTT assay.

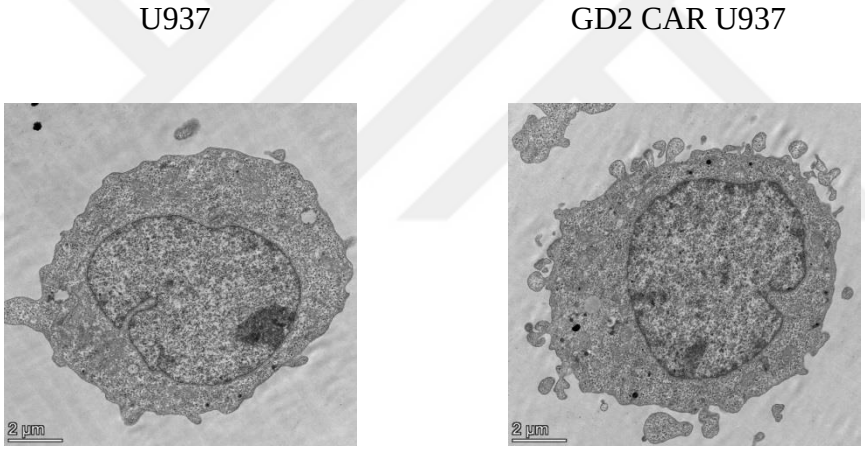

Figure 40: Images of GD2 CAR U937 TEM analysis.

5. DISCUSSION AND CONCLUSION

Due to the low success rate of CAR T cell therapy in solid tumors, the search for new therapeutic options has emerged. It has gained importance to develop an effective cellular therapy method especially in cancer types with high mortality rates in childhood, such as neuroblastoma. Macrophages and monocytes are professional phagocytosing cells, due to their tumor-infiltrating properties and they have great potential for solid tumor treatment. Although the PBMC-derived CAR macrophage production, which is the starting point of this project, is effective in many respects, new cellular therapy alternatives have been proposed at points such as production difficulties (29). In our previous study, a difference was observed between the macrophage differentiation capacity, produced from four different healthy donors. This result shows us that the activity of CAR macrophage produced on a patient basis may vary from donor to donor and a standard activity cannot be obtained.

Due to its nature, macrophage attacks the lentivirus and reduces the efficiency of transduction. The appropriate transduction protocol for macrophages was previously optimized in Labcell. In this context, transduction with lentivirus at different MOIs (1,3,5,10) and transduction methods in the cold environment was tested, and incubation with 5 MOI virus at room temperature was found as the optimal method. In this context, the use of Vectofusin, which is a peptide that increases the transduction efficacy, with 5 MOI virus was the most effective amount in macrophage transduction. Vectofusin, was already shown to increase the transduction efficiency of T cells; the macrophage, NK-92, Hassasin was observed to be effective and non-toxic in U937 cells.

For the tracking and selection of CAR positive cells, EFGRt protein transferred with plasmid was not suitable for macrophages and monocytes (U937), and since these cells naturally express EGFR, CAR tracking could not be performed for these

cell groups (54). For this purpose, first, all Fc receptors were blocked, and then the Fab region of the CAR construct was stained to provide CAR tracking.

After incubation of the produced CAR macrophage with the tumor for 48 hours, an effective tumor-killing capacity emerged with a superior Th1 anti-tumor cytokine response. However, this effect was not statistically significant due to the small group size compared to non-transduced macrophage. In addition, it is thought that the activity of CAR macrophage will increase if the signal domains (MEGF10, BAI) that will increase the phagocytosis efficiency of the macrophage are added to the CAR construct as a cytoplasmic co-domain.

One of the challenges of this study was to produce CAR macrophages with M1 character from PBMC-derived monocyte. Macrophages do not circulate in the bloodstream; hence they cannot be purified expediently in large quantities. Instead, macrophages must be differentiated ex vivo from circulating monocytes by culturing in the presence of human serum or growth factors. Studies have shown that when macrophage cells are trypsinized, their phagocytosis properties are reduced (55). Therefore, the culture process of these cells is difficult. Considering that macrophage does not proliferate like a T cell or a cell line, it seems difficult to reach effective macrophage numbers in individual patient treatment. Due to these challenges of CAR macrophage production, we focused on better effector cell options that would be more applicable in clinical practice. In this context, a series of efficacy and safety analyzes were performed after transduction of NK-92, Hassasin, and U937 cell lines with the same GD2 CAR lentivirus. Our data showed that Hassasin cells, the IL-12 expressing form of NK-92 cells, becomes more effective after CAR transduction. As a result of IL-12 triggering adaptive immunity, PBMC cells in the environment were activated and a Th1 cytokine response was formed. As a result of the comparison of the experimental group with added PBMC with the experimental group without PBMC, there was no increase in tumor-killing capacity, although an increased aggressive cytokine response was detected in 48 hours. This might be due to the need

for more incubation time for the activated PBMC cells to fully activate and attack the tumor, so additional time points can be added to determine the complete profile. When it comes to immunity, in vitro studies are inadequate and lacking in reflecting real human immunity. Therefore, the real-life results of the activated immunity we see in vitro, will be more clearly demonstrated in the in vivo studies.

It has been shown that the anti-tumor capacity of GD2 CAR Hassasin cells, which remain viable for 48 hours after 1000 Gy irradiation, effectively protects the tumor-killing ability thanks to our effective CAR construct. CD16 expression, which is another advantage of Hassasin cells, could not be demonstrated in this thesis study. It is thought that the antibody to be given to the patient within the scope of Anti-GD2 Monoclonal antibody treatment will adhere to CD16 and will create a more effective ADCC response and increase the success of the treatment. As a result, it has been shown that GD2 CAR Hassasin, which is the most effective effector among NK-92 cells, not only kills the tumor cell but also stimulates the immune system by IL-12 secretion, and we can predict that if it is used together with mAb treatment, it will increase the success rate of the treatment. CAR Hassasin has potential for clinical application as itself is a ready-to-use treatment option thanks to the safety of manufacturing.

Considering all these results, we believe that GD2 CAR Hassasin may be an effective bridging therapy in cases of GD2 positive neuroblastoma.

Returning to macrophages, which is the starting point of the thesis, as an off-the-shelf treatment that can facilitate CAR macrophage production, the efficacy of the U937 cell line after CAR transduction has been tested and a patent application has been filed (PT2021-00889). U937s, a monocyte cell line, was found to be advantageous due to infiltrating the tumor and inducing differentiation into M1 macrophages and phagocytosis when it confronts with tumor.

The sterility of the produced GD2 CAR U937 cells has been proven by many parameters. The absence of any cytopathic effect on MSC was demonstrated in the MTT test and microscope images. To confirm that there are no significant side effects in the use of cell lines in cellular therapy methods, control parameters and product safety must be tested. In this context, there should be no pathogenic agent in the treatment product. To test this, the theopathic treatment agent was brought into lysate form and incubated with somatic cells (MSCs) for a long time. The absence of any cytopathic, toxic effects on somatic cells indicated that this product was pathogen-free and safe. In addition, the fact that no viral findings were found in the TEM analysis of the cells in a culture supported the safety of the product.

It was observed that after 1000 Gy irradiation, the cell number and viability were more stable than the NK-92 and Hassasin group. After the analysis, the tumor loses its killing capacity on the 4th day after irradiation, which is quite sufficient and advantageous. However, to safely increase the tumor-killing capacity after irradiation, intensities less than 1000 Gy irradiation can also be tested.

The increased tumor-killing capacity of U937s with the GD2 CAR design is supported by the induced Th1 type cytokine response. Especially since it activates CD8a and increases their granulation, it is effective against GD2 sensitivity. It is obvious that these cells, which are suspended and can multiply indefinitely, are advantageous in terms of clinical applications.

Among all the groups compared in this thesis (Table 9), the most optimal GD2 CAR effector cell group was U937. The clinical simulation should be done by testing these data with in vivo animal models. If efficacy is seen in vivo, it will be an easy-to-produce, effective bridge treatment that can quickly enter clinical practice. Also, it is thought that different CAR constructs can be designed and an increased killing capacity can be obtained by inserting domains that increase phagocytosis in CAR

U937 cells to the cytoplasmic region. These findings are also promising for solid tumors other than neuroblastoma.

This is one of the first studies demonstrating GD2 Neuroblastoma-specific CAR treatment with promising results.

In summary with this thesis;

- An effective and safe CAR construct has been developed.
- Designed CAR was effective in different types of cells.
- It was successful in tumor recognition and killing.

Table 9: Comparison of GD2 CAR effector cells.

	PBMC-derived CAR macrophage	CAR NK-92	CAR Hassasin	CAR U937
Source of donor	Donor specific	Off the shelf	Off the shelf	Off the shelf
Tumor-killing capacity	+ +	+	+ +	+ +
Standardization of effectiveness		+ + +	+ + +	+ + +
Adaptive immunity stimulation	+ +	+ +	+ + +	+ + +
Circulation time in the body		+	+	+ +
Ease of production		+ + +	+ + +	+ + +
Cost	+ + +	+	+	+

6. REFERENCES

1. Voeller J, Sondel PM. Advances in anti-GD2 immunotherapy for treatment of high-risk neuroblastoma. J Pediatr Hematol Oncol. 2019;41(3):163–9.

2. Muenst S, Läubli H, Soysal SD, Zippelius A, Tzankov A, Hoeller S. The immune system and cancer evasion strategies: Therapeutic concepts. J Intern Med. 2016;279(6):541–62.

3. Umut Ö, Gottschlich A, Endres S, Kobold S. CAR T cell therapy in solid tumors: a short review. Memo - Mag Eur Med Oncol. 2021;14(2):143–9.

4. Hou AJ, Chen LC, Chen YY. Navigating CAR-T cells through the solid-tumour microenvironment. Nat Rev Drug Discov [Internet]. 2021;20(July):531–50. Available from: http://dx.doi.org/10.1038/s41573-021-00189-2

5. Marofi F, Motavalli R, Safonov VA, Thangavelu L, Yumashev AV, Alexander M, et al. CAR T cells in solid tumors: challenges and opportunities. Stem Cell Res Ther. 2021;12(1):1–16.

6. Mitwasi N, Feldmann A, Arndt C, Koristka S, Berndt N, Jureczek J, et al. "UniCAR"-modified off-the-shelf NK-92 cells for targeting of GD2-expressing tumour cells. Sci Rep. 2020;10(1):1–16.

7. Vinay DS, Ryan EP, Pawelec G, Talib WH, Stagg J, Elkord E, et al. Immune evasion in cancer: Mechanistic basis and therapeutic strategies. Vol. 35, Seminars in Cancer Biology. Academic Press; 2015. p. S185–98.

8. Heck JE, Ritz B, Hung RJ, Hashibe M, Boffetta P. The epidemiology of neuroblastoma: A review. Paediatr Perinat Epidemiol. 2009;23(2):125–43.

9. Imaizumi M. Recent advances in neuroblastoma research. Seikagaku. 2004;76(5):453–6.

10. Lonergan GJ, Schwab CM, Suarez ES, Carlson CL. From the archives of the AFIP - Neuroblastoma, ganglioneuroblastoma, and ganglioneuroma: Radiologic-pathologic correlation. Radiographics. 2002;22(4):911–34.

11. Sarnacki S, Pio L. Neuroblastoma Clinical and Surgical Management [Internet]. Sarnacki S, Pio L, editors. 2020. 1–57 p. Available from: https://doi.org/10.1007/978-3-030-18396-7

12. Berthold F, Spix C, Kaatsch P, Lampert F. Incidence, Survival, and Treatment of Localized and Metastatic Neuroblastoma in Germany 1979–2015. Pediatr Drugs. 2017;19(6):577–93.

13. Whittle SB, Smith V, Doherty E, Zhao S, McCarty S, Zage PE. Overview and recent advances in the treatment of neuroblastoma. Expert Rev Anticancer Ther [Internet]. 2017;17(4):369–86. Available from: http://dx.doi.org/10.1080/14737140.2017.1285230

14. Johnsen JI, Dyberg C, Wickström M. Neuroblastoma—A neural crest derived embryonal malignancy. Front Mol Neurosci. 2019;12(January):1–11.

15. M.A. Hayat. Diagnosis, Therapy, and Prognosis. 1st ed. 1377.

16. Shimada H. NEUROBLASTOMA – PRESENT AND FUTURE. 2012. 376 p.

17. Sokol E, Desai A. The Evolution of Risk Classification for Neuroblastoma. Children. 2019;6(2):27.

18. Sait S, Modak S. Anti-GD2 immunotherapy for neuroblastoma. Expert Rev Anticancer Ther. 2017;17(10):889–904.

19. Nazha B, Inal C, Owonikoko TK. Disialoganglioside GD2 Expression in Solid Tumors and Role as a Target for Cancer Therapy. Front Oncol. 2020;10(July):1–15.

20. Kholodenko I V., Kalinovsky D V., Doronin II, Deyev SM, Kholodenko R V. Neuroblastoma origin and therapeutic targets for immunotherapy. J Immunol Res. 2018;2018.

21. Gonzalez H, Hagerling C, Werb Z. Roles of the immune system in cancer: From tumor initiation to metastatic progression. Genes Dev. 2018;32(19–20):1267–84.

22. Taştan C, Kançağı DD, Turan RD, Yurtsever B, Çakırsoy D, Abanuz S, et al. Preclinical Assessment of Efficacy and Safety Analysis of CAR-T Cells (ISIKOK-19) Targeting CD19-Expressing B-Cells for the First Turkish Academic Clinical Trial with Relapsed/Refractory ALL and NHL Patients. Turkish J Haematol Off J Turkish Soc Haematol. 2020;37(4):234–47.

23. Ma S, Li X, Wang X, Cheng L, Li Z, Zhang C, et al. Current progress in car-t cell therapy for solid tumors. Int J Biol Sci. 2019;15(12):2548–60.

24. Maude SL, Laetsch TW, Buechner J, Rives S, Boyer M, Bittencourt H, et al. Tisagenlecleucel in Children and Young Adults with B-Cell Lymphoblastic Leukemia. N Engl J Med. 2018;378(5):439–48.

25. Ali S, Kjeken R, Niederlaender C, Markey G, Saunders TS, Opsata M, et al. The European Medicines Agency Review of Kymriah (Tisagenlecleucel) for the Treatment of Acute Lymphoblastic Leukemia and Diffuse Large B-Cell Lymphoma. Oncologist. 2020;25(2).

26. Li X, Liu R, Su X, Pan Y, Han X, Shao C, et al. Harnessing tumor-associated macrophages as aids for cancer immunotherapy. Mol Cancer. 2019;18(1):1–16.

27. Kershaw MH, Westwood JA, Parker LL, Wang G, Eshhar Z, Mavroukakis SA, et al. A phase I study on adoptive immunotherapy using gene-modified T cells for ovarian cancer. Clin Cancer Res [Internet]. 2006 Oct 15 [cited 2019 Oct 30];12(20 Pt 1):6106–15. Available from: http://www.ncbi.nlm.nih.gov/pubmed/17062687

28. Zhang C, Oberoi P, Oelsner S, Waldmann A, Lindner A, Tonn T, et al. Chimeric antigen receptor-engineered NK-92 cells: An off-the-shelf cellular therapeutic for targeted elimination of cancer cells and induction of protective antitumor immunity. Front Immunol. 2017;8(MAY).

29. Weiskopf K, Weissman IL. Macrophages are critical effectors of antibody therapies for cancer. MAbs. 2015;7(2):303–10.

30. Mosser DM, Edwards JP. Exploring the full spectrum of macrophage activation. Nat Rev Immunol [Internet]. 2008;8(12):958–69. Available from: http://dx.doi.org/10.1038/nri2448

31. Hirayama D, Iida T, Nakase H. The phagocytic function of macrophage-enforcing innate immunity and tissue homeostasis. Int J Mol Sci. 2018;19(1).

32. Mosser DM, Edwards JP. Nihms84393. Nat Rev Immunol. 2009;8(12):958–69.

33. Karavitis J, Kovacs EJ. Macrophage phagocytosis: effects of environmental pollutants, alcohol, cigarette smoke, and other external factors. J Leukoc Biol. 2011;90(6):1065–78.

34. Klichinsky M, Ruella M, Shestova O, Lu XM, Best A, Zeeman M, et al. Human chimeric antigen receptor macrophages for cancer immunotherapy. Nat Biotechnol. 2020;38(8):947–53.

35. Kumar V. Macrophages: The Potent Immunoregulatory Innate Immune Cells. Macrophage Act - Biol Dis. 2020;

36. Weiskopf K, Weissman IL. Macrophages are critical effectors of antibody therapies for

cancer. [cited 2020 Jun 16]; Available from: http://dx.doi.org/10.1080/19420862.2015.1011450

37. Poltavets AS, Vishnyakova PA, Elchaninov A V., Sukhikh GT, Fatkhudinov TK. Macrophage Modification Strategies for Efficient Cell Therapy. Cells. 2020;9(6):1–19.

38. Smith JD. Human Macrophage Genetic Engineering. Arterioscler Thromb Vasc Biol. 2016;36(1):2–3.

39. Carisma Therapeutics [Internet]. 2021. Available from: https://carismatx.com/

40. Morrissey MA, Williamson AP, Steinbach AM, Roberts EW, Kern N, Headley MB, et al. Chimeric antigen receptors that trigger phagocytosis. Elife. 2018 Jun 4;7.

41. Suck G, Odendahl M, Nowakowska P, Seidl C, Wels WS, Klingemann HG, et al. NK-92: an 'off-the-shelf therapeutic' for adoptive natural killer cell-based cancer immunotherapy. Cancer Immunol Immunother. 2016;65(4):485–92.

42. Klingemann H, Boissel L, Toneguzzo F. Natural killer cells for immunotherapy - Advantages of the NK-92 cell line over blood NK cells. Front Immunol. 2016;7(MAR):1–7.

43. Luo H, Wu X, Sun R, Su J, Wang Y, Dong Y, et al. Target-Dependent Expression of IL-12 by synNotch Receptor-Engineered NK-92 Cells Increases the Antitumor Activities of CAR-T Cells. Front Oncol. 2019;9(December):1–11.

44. Colombo MP, Trinchieri G. Interleukin-12 in anti-tumor immunity and immunotherapy. Cytokine Growth Factor Rev. 2002;13(2):155–68.

45. Ferrara C, Grau S, Jaëger C, Sondermann P, Brunker P, Waldhauer I, et al. Unique carbohydrate-carbohydrate interactions are required for high affinity binding between FcγRIII and antibodies lacking core fucose. Proc Natl Acad Sci U S A. 2011;108(31):12669–74.

46. Camilo Galindo C, Arturo Clavijo-Ramírez C. Generation and characterization of U937-TR: A platform cell line for inducible gene expression in human macrophages. Parasitology. 2020;147(13):1524–31.

47. Verhoeckx K, Cotter P, López-Expósito I, Kleiveland C, Lea T, Mackie A, et al. The impact of food bioactives on health: In vitro and Ex Vivo models. Impact Food Bioact Heal Vitr Ex Vivo Model. 2015;1–327.

48. Zhang WJ, Zhang WG, Zhang PY, Cao XM, He AL, Chen YX, et al. The expression and functional characterization associated with cell apoptosis and proteomic analysis of the novel gene MLAA-34 in U937 cells. Oncol Rep. 2013;29(2):491–506.

49. Esser R, Müller T, Stefes D, Kloess S, Seidel D, Gillies SD, et al. NK cells engineered to express a GD 2-specific antigen receptor display built-in ADCC-like activity against tumour cells of neuroectodermal origin. J Cell Mol Med. 2012;16(3):569–81.

50. Shaqireen Kwajah MM, Schwarz H. CD137 ligand signaling induces human monocyte to dendritic cell differentiation. Eur J Immunol. 2010;40(7):1938–49.

51. Jiang D, Chen Y, Schwarz H. CD137 Induces Proliferation of Murine Hematopoietic Progenitor Cells and Differentiation to Macrophages. J Immunol. 2008;181(6):3923–32.

52. Wang X, Chang WC, Wong CLW, Colcher D, Sherman M, Ostberg JR, et al. A transgene-encoded cell surface polypeptide for selection, in vivo tracking, and ablation of engineered cells. Blood. 2011;118(5):1255–63.

53. Taştan C, Yurtsever B, Sir Karakuş G, Dilek Kançağı D, Demir S, Abanuz S, et al. SARS-CoV-2 isolation and propagation from turkish COVID-19 patients. Turkish J Biol.

2020;44(Special issue 1):192–202.

54. Lamb DJ, Modjtahedi H, Plant NJ, Ferns GAA. EGF mediates monocyte chemotaxis and macrophage proliferation and EGF receptor is expressed in atherosclerotic plaques. Atherosclerosis. 2004;176(1):21–6.

55. Chen S, So EC, Strome SE, Zhang X. Impact of Detachment Methods on M2 Macrophage Phenotype and Function. J Immunol Methods [Internet]. 2015;426:56–61. Available from: http://dx.doi.org/10.1016/j.jim.2015.08.001

7. APPENDICES

Appendix 1: Mesenchymal Stem Cell Donor Consent Form.

Appendix 1: Mesenchymal Stem Cell Donor Consent Form (Continue).

Appendix 1: Mesenchymal Stem Cell Donor Consent Form (Continue).

Appendix 1: Mesenchymal Stem Cell Donor Consent Form (Continue).

Appendix 1: Mesenchymal Stem Cell Donor Consent Form (Continue).

Appendix 1: Mesenchymal Stem Cell Donor Consent Form (Continue).

Appendix 2: Ethics Committee Approval and Voluntary Consent Form.

Appendix 2: Ethics Committee Approval and Voluntary Consent Form (continue).

Appendix 2: Ethics Committee Approval and Voluntary Consent Form (continue).

Appendix 2: Ethics Committee Approval and Voluntary Consent Form (continue).

Appendix 2: Ethics Committee Approval and Voluntary Consent Form (continue).

Appendix 3: Supplementary data

	Only MSC	U937	GD2 CAR U937
DAY 1	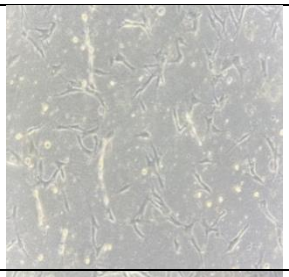	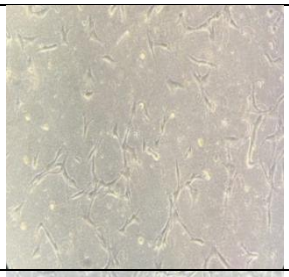	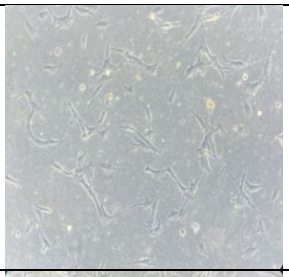
DAY 2	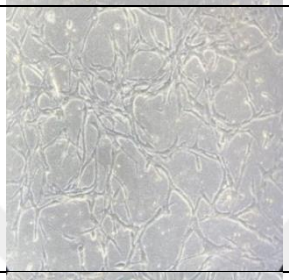	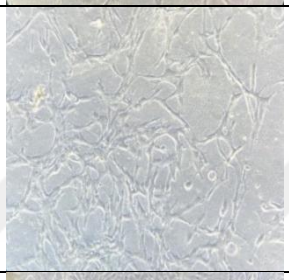	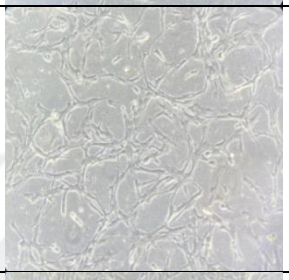
DAY 3	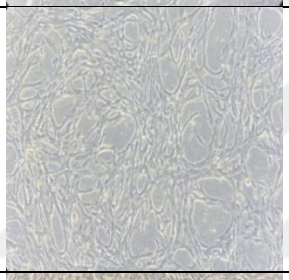	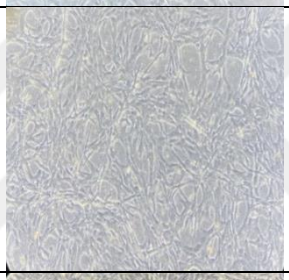	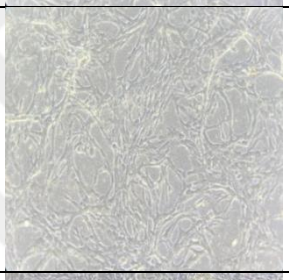
DAY 4	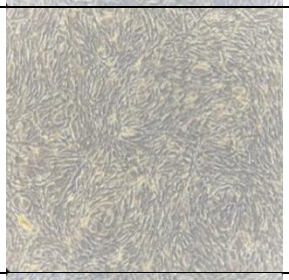	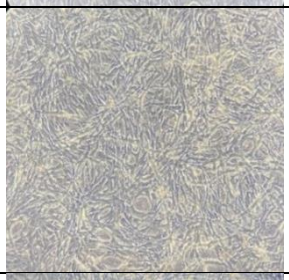	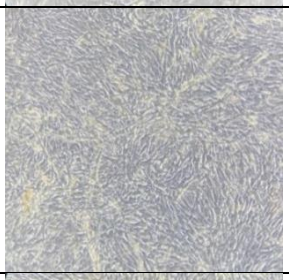
DAY 7	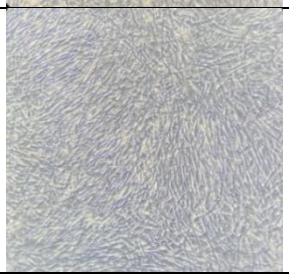	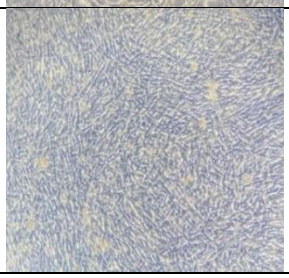	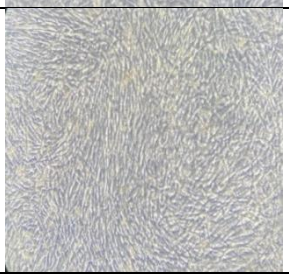

Supplementary figure: Light microscopy result of 7-day cytopathic effect analysis of MSC cells incubated with cell lysates.

8. CURRICULUM VITAE